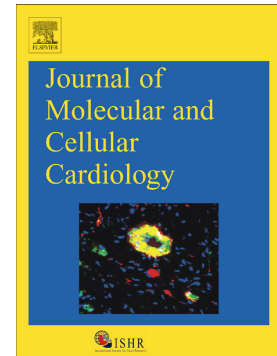


Accepted Manuscript

Altered long non-coding RNA expression profile in rabbit atria with atrial fibrillation: TCONS_00075467 modulates atrial electrical remodeling by sponging miR-328 to regulate CACNA1C

Zhan Li, Ximin Wang, Weizong Wang, Juanjuan Du, Jinqiu Wei, Yong Zhang, Jiangrong Wang, Yinglong Hou



PII: S0022-2828(17)30106-2
DOI: doi: [10.1016/j.yjmcc.2017.05.009](https://doi.org/10.1016/j.yjmcc.2017.05.009)
Reference: YJMCC 8547

To appear in: *Journal of Molecular and Cellular Cardiology*

Received date: 17 November 2016
Revised date: 17 May 2017
Accepted date: 19 May 2017

Please cite this article as: Zhan Li, Ximin Wang, Weizong Wang, Juanjuan Du, Jinqiu Wei, Yong Zhang, Jiangrong Wang, Yinglong Hou , Altered long non-coding RNA expression profile in rabbit atria with atrial fibrillation: TCONS_00075467 modulates atrial electrical remodeling by sponging miR-328 to regulate CACNA1C. The address for the corresponding author was captured as affiliation for all authors. Please check if appropriate. Yjmcc(2017), doi: [10.1016/j.yjmcc.2017.05.009](https://doi.org/10.1016/j.yjmcc.2017.05.009)

This is a PDF file of an unedited manuscript that has been accepted for publication. As a service to our customers we are providing this early version of the manuscript. The manuscript will undergo copyediting, typesetting, and review of the resulting proof before it is published in its final form. Please note that during the production process errors may be discovered which could affect the content, and all legal disclaimers that apply to the journal pertain.

Altered long non-coding RNA expression profile in rabbit atria with atrial fibrillation: TCONS_00075467 modulates atrial electrical remodeling by sponging miR-328 to regulate CACNA1C

Zhan Li, Ximin Wang, Weizong Wang, Juanjuan Du, Jinqiu Wei, Yong Zhang, Jiangrong Wang, Yinglong Hou*

From the Department of Cardiology, Shandong Provincial Qianfoshan Hospital, Shandong University, Jinan 250014, P.R. China

*Correspondence to Dr. Yinglong Hou;

Address: Department of Cardiology, Shandong Provincial Qianfoshan Hospital, Shandong University, No. 16766 Jingshi Road, 250014, Jinan City, China;

Telephone /Fax: +86-531-89269217;

E-mail: yinglonghou@hotmail.com

Abstract

Electrical remodeling has been reported to play a major role in the initiation and maintenance of atrial fibrillation (AF). Long non-coding RNAs (lncRNAs) have been increasingly recognized as contributors to the pathology of heart diseases. However, the roles and mechanisms of lncRNAs in electrical remodeling during AF remain unknown. In this study, the lncRNA expression profiles of right atria were investigated in AF and non-AF rabbit models by using RNA sequencing technique and validated using quantitative real-time polymerase chain reaction (qRT-PCR). A total of 99,843 putative new lncRNAs were identified, in which 1220 differentially expressed transcripts exhibited more than 2-fold change. Bioinformatics analysis was conducted to predict the functions and interactions of the aberrantly expressed genes. On the basis of a series of filtering pipelines, one lncRNA, TCONS_00075467, was selected to explore its effects and mechanisms on electrical remodeling. The atrial effective refractory period was shortened *in vivo* and the L-type calcium current and action potential duration were decreased *in vitro* by silencing of TCONS_00075467 with lentiviruses. Besides, the expression of miRNA-328 was negatively correlated with TCONS_00075467. We further demonstrated that TCONS_00075467 could sponge miRNA-328 *in vitro* and *in vivo* to regulate the downstream protein coding gene CACNA1C. In addition, miRNA-328 could partly reverse the effects of TCONS_00075467 on electrical remodeling. In summary, dysregulated lncRNAs may play important roles in modulating electrical remodeling during AF. Our study may facilitate the mechanism studies of lncRNAs in AF pathogenesis and provide potential therapeutic targets for AF.

Keywords: atrial fibrillation, atrial electrical remodeling, long non-coding RNA, TCONS_00075467.

1. Introduction

Atrial fibrillation (AF), one of the most common arrhythmias, increases the risk of heart failure and ischemic stroke, and contributes substantially to disease-related morbidity and mortality [1, 2]. AF is characterized by atrial electrical remodeling and structural remodeling, which are mainly mediated by ion-channel alterations and fibrosis/apoptosis respectively [3-5], and favor arrhythmia recurrence and maintenance [6, 7]. Atrial electrical remodeling occurs both in left and right atrium at the early stage of AF and leads to the shortening of atrial effective refractory period (AERP) and action potential duration (APD), which can facilitate the initiation of AF and other remodeling. The effects of left atrial remodeling on the initiation of AF have been identified [4, 7]. But the roles and mechanisms of right atrial electrical remodeling in AF have not been illustrated thoroughly. Previous reports suggest that genetic factors play a pivotal role in electrical remodeling in AF [8, 9].

Long non-coding RNAs (lncRNAs) are generally defined as non-protein coding RNAs with more than 200 nucleotides (nt) in length [10]. LncRNAs may function through a variety of mechanisms, including chromatin remodeling, genomic imprinting, splicing regulation, and mRNA decay [11]. LncRNAs also affect microRNA (miRNA, miR) functions by controlling pre-miRNA splicing or as miRNA sponges [12]. Recently, mounting evidences reveal that differently expressed lncRNAs play indispensable roles in many heart diseases, including heart failure, cardiac hypertrophy and AF [13-15]. Although lncRNAs have been studied in the pathogenesis of AF [16, 17], their roles and mechanisms in electrical remodeling during AF have not been investigated.

In order to identify the influence of right atrial electrical remodeling on AF and the roles of lncRNAs in electrical remodeling during AF, the lncRNA expression profiles of right atria (RA) in rabbit AF models were investigated by using high-throughput RNA sequencing (RNA-Seq), and the electrical remodeling related lncRNA was identified. Then the electrophysiology and electrical remodeling were examined in RA and primary atrial cardiomyocytes after knockdown of the novel lncRNA. Furthermore the mechanisms of the lncRNA in the pathogenesis of electrical remodeling in AF were explored. It will help to illustrate the molecular pathogenesis of AF and find new therapeutic targets for AF.

2. Materials and Methods

2.1 Ethics statement

The study was approved by the Ethics Committee of Shandong Provincial Qian Foshan Hospital, Shandong University, in Jinan, China. The protocols used in this study were in compliance with the Guidelines for the Care and Use of Laboratory Animals published by the National Academy Press (NIH publication No. 85-23, revised 1996).

2.2 Animal preparation

Twelve adult New Zealand white rabbits weighing about 3 kg of male or female sex were randomly divided into two groups: AF (n=6) and control (n=6). The AF group underwent continuous atrial tachypacing (600 beats/min) for 1 week. The rabbits were anesthetized with 30 mg/kg of intravenous pentobarbital Na. Four

electrode endocardial leads attached to pacemakers (AOP, Fudan University, Shanghai, China) were inserted into the right atrial appendage via right jugular veins under X-ray guidance. The pacemakers were implanted in subcutaneous pockets to achieve permanent pacing. The control group was sham-operated in the same way as the AF group without pacing. AERP and AF inducibility were determined before pacing and 7 d after pacing. Programmed electrical stimulation (PES) was conducted by placing a electrophysiological catheter into the right atrium via right jugular vein using Electrophysiology Management System of LEAD-7000 (Jinjiang Electronic Science and Technology, Sichuan, China). The procedures were as described by us [18]. Rapid irregular atrial rhythms lasting >30 s were regarded as successful inductions of AF.

2.3 Tissue processing

After 1 week of continuous pacing, all animals were euthanized by air embolism. RA were obtained from all animals and the samples were stored at -80°C until use.

2.4 Primary atrial cardiomyocytes culture

The chest cavities of male or female rabbits were opened within 24 h after birth, and the hearts were removed and placed in chilled phosphate buffered saline. After washing, the upper part of the hearts were cut into 1 mm³ pieces with scissors and then digested by 3 ml of 0.1% collagenase II (Solarbio, Beijing, China). After digestion, the supernatant was dissolved in high glucose DMEM (Hyclone, Logan, Utah) containing 10% fetal bovine serum (CLARK, Richmond, VA) to terminate digestion, and this procedure was repeated five times. The product was centrifuged at 1,000 rpm for 5 min. The supernatant was discarded and the cells were resuspended in a culture flask and placed in a 37 °C 5% CO₂ incubator. Cardiomyocytes were separated from fibroblast cells by means of differential adhesion technique [19]. After 24 h, the medium was changed.

2.5 High-throughput RNA-Seq

According to the manufacturer's protocol, total RNAs were isolated from the RA of each sample (three samples in control group, and three samples in AF group) by using TRIzol reagent (Invitrogen, Carlsbad, CA). The RNA concentration of each sample was determined by measuring the absorption at 260 and 280 nm using a SMA1000 ultraviolet spectrophotometer (Merinton, Beijing, China).

High-throughput RNA-Seq of the six samples was performed on Illumina Hiseq 2500 with a 50 base pair single-end protocol (Illumina, San Diego, CA). The bioinformatics analysis was performed as described previously [17, 20]. Candidate lncRNAs were acquired by satisfying the following criteria: RNA length ≥ 200 nt, Coding Potential Calculator (CPC) score ≤ 0 , Coding-Potential Assessment Tool (CPAT) probability ≤ 0.364 , and phylogenetic analysis of Codon Substitution Frequencies (phyloCSF) score ≤ -20 .

The expression levels of the transcripts were calculated by fragments per kilobase of transcript per million fragments mapped (FPKM) values. Differentially expressed

transcripts (DETs) were defined as $p < 0.05$ and fold change > 2 times based on their FPKM values between the groups, which were identified using Cuffdiff software.

2.6 Quantification analysis of RNA

Reverse-transcribed cDNA was synthesized by 1 μg of total RNA using RevertAid First Strand cDNA Synthesis Kit (Thermo, Vilnius, Lithuania). Quantitative real-time PCR (qRT-PCR) analysis was conducted with Maxima SYBR Green/ROX qPCR Master Mix (2X) (Thermo, Vilnius, Lithuania) on the ABI ViiA 7 Real-Time PCR system (Applied Biosystems, Foster City, CA). And the quantification of miRNAs was used by All-in-One miRNA qRT-PCR Detection Kit (GeneCopoeia, Rockville, MD). Each sample was tested in triplicate. The relative gene expression levels were calculated using $2^{-\Delta\Delta\text{Ct}}$ method against GAPDH or U6 for standardization. Then the RNA was reverse-transcribed to unique cDNA by using Taq Master Mix (TIANGEN, Beijing, China) with specific primer on the ABI GeneAmp PCR system 9700 (Applied Biosystems, Singapore). After 30-35 cycle, agarose gel electrophoresis was conducted with these cDNA mixtures to reflect the expression and abundance of RNA. The gene-specific primers used for amplification are listed in Table A.1.

2.7 GO and KEGG pathway analysis

Gene ontology (GO) was adopted to annotate the functions of differentially expressed genes in the GO vocabularies. Briefly, the differentially expressed genes were regarded as candidates from the whole genes. The enrichment p -value was confirmed between the GO feature sets and the differentially expressed genes were calculated using a hypergeometric distribution test. The p -value was further corrected by Benjamini–Hochberg multiple test to obtain the false discovery rate (FDR). Based on p -value and FDR, the enrichment score was expressed in $-\log_{10}(p\text{-value})$. Kyoto Encyclopedia of Genes and Genomes (KEGG) pathway analysis was also applied to define the functions of the differentially expressed genes in graphical diagrams of biochemical pathways. KEGG pathway analysis was similar to that of GO functional analysis. The significance was calculated by p -value and FDR.

2.8 Target gene prediction

Cis- and trans-predictions were used to identify the target genes of the differentially expressed lncRNAs. For cis-prediction, a systematic search was performed based on the genomic location of the lncRNAs to identify the known protein-coding transcripts. The interaction categories and prediction methods were described previously [17]. For trans-prediction, Basic Local Alignment Search Tool (BLAST) sequence comparison between the lncRNAs and 3' untranslated regions (UTR) of the known protein-coding transcripts was performed to assess the possibility of forming complexes. The criteria of the BLAST sequence analysis indicated that the ratio between the target and query sequence lengths should be $> 10\%$.

2.9 Coexpression network

Subsequently, a coexpression network was constructed among the significantly differential expressed lncRNAs and coding genes by Pearson's correlation coefficients, which equal to or greater than 0.85 [21, 22]. In the network, a blue node represents a lncRNA and a red node represents a mRNA. A black line represents a positive correlation, and a green line represents a negative correlation.

2.10 Interaction network between lncRNA and miRNA

Based on the lncRNA sequences and the miRNA expression profile in AF model [23-27], the starBase v2.0, PITA, MIRDB4.0 and NCBI blast database were used to predict the binding sites between lncRNA and miRNA. The target genes of associated miRNAs were predicted according to TargetScan and RegRNA 2.0 database. Then the gene interference was implemented to verify the interaction between the target lncRNA and miRNA, and identify their functions in cardiomyocytes.

2.11 Silencing of TCONS_00075467

Four small interfering RNA (siRNA) for inhibiting TCONS_00075467 were synthesized by GenePharma (GenePharma, Shanghai, China). The siRNA sequences are listed in Table A.2. Two days after extraction, the primary myocytes were planked in 6-wells plates (2×10^5 /well) and randomly divided into three groups: blank control group, negative control group cultured with 75 pmol negative RNA oligo, anti-TCONS_00075467 group cultured with 75 pmol siRNA targeting TCONS_00075467. The siRNA was transfected using 10 μ l Lipofectamine 2000 (Invitrogen, Carlsbad, CA), and the blank control group was also cultured with the same amount of Lipofectamine 2000. The RNA was extracted from the cultured cells after 48 h to test their inhibiting efficiency.

2.12 Construction of lentiviruses

Negative short hairpin RNA (shRNA) (negative control) and four siRNAs in one shRNA targeting TCONS_00075467 (RNAi-TCONS_00075467) were designed by ViGene (ViGene Biosciences, Rockville, MD). Negative shRNA (negative control), ocu-miR-328 precursor shRNA (miR-328 mimics) and anti-miR-328 antisense shRNA (miR-328 inhibitor) were designed by GenePharma. The shRNA sequences are listed in Table A.2. The procedures about construction of lentiviruses were as described by us [17]. Finally the recombinant lentiviral vectors were obtained with a titer of 1×10^9 TU/ mL for injection.

2.13 Infection of lentiviruses

Two days after extraction, the primary myocytes were planked in 6-wells plates (2×10^5 /well) and randomly divided into six groups: blank control group, negative control group cultured with 40 μ l negative lentiviruses, lenti-RNAi-TCONS_00075467 group cultured with 40 μ l lentiviruses targeting TCONS_00075467, lenti-miR-328 inhibitor group cultured with 40 μ l lentiviruses inhibiting ocu-miR-328, lenti-miR-328 mimics group cultured with 40 μ l lentiviruses containing ocu-miR-328 precursor shRNA, and co-infected lentiviruses group cultured with 40 μ l lentiviruses targeting TCONS_00075467 and 40 μ l lentiviruses inhibiting ocu-miR-328. The RNA was extracted from the cultured cells after 96 h and the protein was extracted after 120 h.

Twenty-five adult male or female rabbits were randomly allocated into five groups: (i) negative control (n=5), infected with negative control lentiviruses; (ii) lenti-RNAi-TCONS_00075467 (n=5), infected with lentiviruses targeting TCONS_00075467; (iii) lenti-miR-328 inhibitor (n=5), infected with lentiviruses inhibiting ocu-miR-328; (iv)

lenti-miR-328 mimics (n=5), infected with lentiviruses containing ocu-miR-328 precursor shRNA; and (v) co-infected lentiviruses group, co-infected with the lentiviruses targeting TCONS_00075467 and the lentiviruses inhibiting ocu-miR-328. The rabbits were anesthetized with 30 mg/kg of intravenous pentobarbital Na. The median thoracotomy was performed and the third and fourth ribs were cut off, then the heart was exposed after excising the pericardium. The RA was fixed, and 150 μ l lentiviruses were directly injected into 10 separate sites through a microsyringe to distribute the transfer vectors uniformly over a large area [28]. Then the heart was replaced into the thoracic cavity, the chest was closed with sutures, and air in the thoracic cavities was evacuated. Samples were collected 7 d after infection. After the animal was euthanized, the heart was immediately excised and perfused. The RA was dissected and frozen in liquid nitrogen for quantification of RNA and protein. The procedures were as described by us [18].

AERP and AF inducibility were measured after thoracotomy (before infection), immediately after infection and 7 d after infection. The procedures were consistent with the descriptions in the front paragraph.

2.14 Western Blot

The protein samples were extracted from the RA of rabbit and cultured primary atrial myocytes with Membrane and Cytosol Protein Extraction Kit (Beyotime, Beijing China). Protein concentration was quantified with a BCA Protein Assay Kit (Beyotime, Beijing, China). The procedures were essentially same as described in detail by us [18]. The PVDF membranes were incubated overnight at 4 °C with diluted antibodies against CACNA1C (1:1000, Abcam, Cambridge, UK), KCND3 (1:1000, Abcam, Cambridge, UK), KCNJ2 (1:800, Proteintech, Wuhan, China), or GAPDH (1:1000, Beyotime, Beijing, China), followed by incubation with an HRP-conjugated secondary antibody (1:10000, Beyotime, Beijing, China). The bands were quantified using ImageJ software (NIH Image) by measuring the band intensity (Area x OD) for each group and normalizing to GAPDH. The final results are expressed as fold change by normalizing the data to the control values.

2.15 Construction of plasmids for luciferase

The ocu-miR-328 mimics and negative control mimics were synthesized by GenePharma. The DNA sequence of the 3'UTR of CACNA1C was acquired from *Oryctolagus cuniculus* cDNA library (NCBI GenBank). The DNA fragments containing the wild type (WT) and mutation type (Mut) sequences of TCONS_00075467 and 3'UTR of CACNA1C were synthesized by GenePharma. The oligonucleotides were ligated into NotI and XhoI sites by T4 Ligase in the psi-CHECK-2 luciferase reporter vectors (Promega, Madison, WI).

2.16 Luciferase activity assay

Reporter assays were conducted using HEK293T cells in 48-well plates in triplicate and replicated 3 times. The 293T were transfected with 40 ng of the reporter vectors and 10 pmol of ocu-miR-328 mimics or negative control mimics with Lipofectamine 2000 in 100 μ l Opti-MEM (Gibco, Grand Island, NY). After 6 h, the Opti-MEM was changed to complete medium. Following transfection of 48 h, luciferase activities were measured with the Dual-Luciferase Reporter Assay System (Promega, Madison, WI) on GloMaxTM 96 Microplate Luminometer (Promega, Madison, WI).

2.17 Whole-cell patch-clamp recording

Patch-clamp techniques were applied to primary myocytes after lentiviruses infected. The procedures have been described in detail elsewhere [29-31]. Briefly, the pipette of patch electrodes had the tip resistance of 3-5 M Ω when filled with pipette solution. The single cells were placed in a 1-ml chamber mounted on an inverted microscope (IX-70, Olympus, Japan) and perfused with Tyrode solution. Whole-cell recording were performed using an amplifier (Axopatch 700B, Axon instrument, Sunnyvale, CA). Signals were filtered at 1 kHz and data were acquired by A/D conversion (Digidata 1550B, Axon Instrument). L-type calcium current (I_{CaL}) was recorded in the whole cell voltage-clamp mode and APD was recorded under the current-clamp mode. The compositions of Tyrode and pipette solutions were listed in Table A.3.

2.18 Fluorescent in situ hybridization (FISH) for detection of TCONS_00075467

FISH for TCONS_00075467 and miR-328 was conducted as previously described [32]. On 4% paraformaldehyde fixed slides with monolayers of primary myocytes, using CY3-labelled probe for TCONS_00075467 and Dylight 488-labelled probe for miR-328 at 5 ng/ μ l concentration. Hybridization was performed at 37 °C overnight, followed by visualization using fluorescence microscope (Nikon, Tochigi, Japan). Slides were subsequently counterstained using DAPI.

2.19 Statistical analysis

Statistical analysis was performed using SPSS 17.0 software (IBM Corp., Armonk, NY). All data were expressed as mean \pm standard error of mean (SEM). For sequencing data, paired-sample t-test was used to compare the expression of lncRNAs. For qRT-PCR data, unpaired t-test was used to compare the gene expression levels between the groups. Comparisons between groups were conducted using one-way analysis of variance (ANOVA) followed by Bonferroni's post hoc test. $p < 0.05$ and $p < 0.01$ were respectively considered statistically significant and highly significant differences for all of the analyses.

3. Results

3.1 AERP decreased in AF models

AF models were successfully established in all rabbits receiving right atrial tachypacing. The electrocardiographs of sinus rhythm and AF are shown in Figure 1A. Compared with the control group, AERP significantly decreased in the AF group (74.2 ± 9.2 vs. 100.8 ± 7.4 , $p < 0.01$) (Fig. 1B). AF was induced in four out of six rabbits, and paroxysmal atrial tachycardia (lasting < 30 s) existed in all six rabbits in the AF group, while in the control group, paroxysmal atrial tachycardia was induced in two rabbits (Fig. 1C). According to the studies on atrial tissue remodeling [33], the relative gene expression of key ion channels were tested in this AF model. Compared with the control group, the expression of CACNA1C and KCND3 in AF group decreased significantly, while the expression of KCNJ2 in AF group increased markedly as validated by Western Blot (Fig. 1D for RA, Fig. A.1 for left atria), which accorded with the expression profile of human and murine models [33, 34].

3.2 Alignment of sequencing reads

Using the Illumina HiSeq 2500 platform, the total raw reads ranged from 51 million to 71 million. TopHat aligner indicated that about 41-57 million reads were uniquely mapped to the *Oryctolagus* genome sequence (Table A.4). No obvious differences regarding the percentage of genomic alignment (AF vs. control: 89.6% vs. 86.8%), and the density distributions of the reference genome among chromosomes were observed, suggesting slight bias in the sequencing results. Repetition of reads was evaluated by two strategies: one was based on identical read sequences and the other was comparable to the corresponding genome location. The distribution of the total mapped reads onto the genome showed that 77.4% were aligned at the exons and UTR regions, 11.3% at the introns, 11.0% at the intergenic regions and others were splicing transcripts (Fig. A.2). Uniform distributions of the transcripts elucidated that the quality of the RNA-Seq was excellent, which was verified by data analysis.

3.3 Analysis of differentially expressed lncRNAs

A total of 99843 putative new lncRNAs were detected, in which 2529 transcripts contained multiple exons. After filtering based on CPC score, CPAT probability, and phyloCSF score, 6083 transcripts were reserved as candidate lncRNAs. Based on FPKM values, 1220 DETs exhibited more than 2-fold change and $p < 0.05$, in which 983 transcripts were down-regulated and 237 were up-regulated. The new lncRNAs were further displayed by heat map (Fig. 2A). A volcano plot elucidated the variance in DETs based on p -value and fold change (Fig. 2B). Correspondingly, the fold changes of the significant DETs are listed in Table 1.

3.4 GO and KEGG pathway analysis

Differentially expressed genes were categorized and annotated by GO functional analysis, which used three structured and controlled vocabularies to describe the gene products in terms of associated biological processes, cellular components and molecular functions. The results showed that the functions of the differentially expressed genes mainly involved the following biological processes: (I) GO:0005509 calcium ion binding; (II) GO:0003700 sequence-specific DNA binding transcription factor activity; (III) GO:0007155 cell adhesion; (IV) GO:0045944 positive regulation of transcription from RNA polymerase II promoter; (V) GO:0008284 positive regulation of cell proliferation; (VI) GO:0030198 extracellular matrix organization and (VII) GO:0055085 transmembrane transport (Fig. 2D).

The KEGG pathway consists of a number of graphical diagrams illustrating the molecular interactions and reaction networks. The KEGG pathway analysis indicated that the differentially expressed genes were enriched in the following pathways: (I) ko04020 calcium signaling pathway; (II) ko05412 arrhythmogenic right ventricular cardiomyopathy; (III) ko05410 hypertrophic cardiomyopathy; (IV) ko05414 dilated cardiomyopathy; (V) ko04540 Gap junction; and (VI) ko01100 metabolic pathways (Fig. 2E).

3.5 Quantification of lncRNAs expression

In order to validate the RNA-Seq results, three down-regulated and three up-regulated lncRNAs were randomly selected from the new DETs. The relative expression levels of these new DETs were analyzed by qRT-PCR in the six samples. The expression trends were consistent with those obtained from the RNA-Seq. The expression of the up-regulated TCONS_00042168, TCONS_00009169,

TCONS_00025394 and the down-regulated TCONS_00072451, TCONS_39902 achieved statistical significance, which were consistent with the RNA-Seq results. While TCONS_00053509 expression had no difference between the groups, which failed to match with the RNA-Seq results (Fig. 3A).

3.6 Identification of candidate lncRNAs

The identification process of candidate lncRNAs in electrical remodeling is described as follows. Firstly, lncRNAs with more than an absolute 2-fold change were selected. Then, the predicted target genes, interacting miRNAs and co-expression mRNAs of DETs associated with atrial electrical remodeling and ion channels were selected. Aiming at the identified lncRNAs and co-expression genes, transcripts conserved matched to human genome, GO and KEGG pathway analyses were also conducted. With these three steps, two down-regulated lncRNAs (TCONS_00075467 and TCONS_00074073) were selected. Finally, considering that lncRNAs were tissue-specific, the expression of the two selected lncRNAs was examined by qRT-PCR in nervous tissue, aorta, skeletal muscle and atrial tissue of rabbits to select atrium-specific lncRNAs (Fig. 3B). The results showed that TCONS_00075467 can be used for further analysis.

3.7 Overview of TCONS_00075467

Sequence analysis using the NCBI BLAST revealed that TCONS_00075467 was located on the forward strand of chromosome 13: 141223079-141225530 (OryCun 2.0), and the transcript belongs to long intergenic ncRNAs (lincRNAs), which do not overlap with any protein-coding loci [35]. This transcript matched to 72% conserved sequence of human genome located in chromosome 1: 8793506-8794286 and chromosome 1: 8798078 to 8798802 (Fig. A.3). Then the open reading frame (ORF) and coding potential analyses were conducted by ORF Finder of NCBI (<http://www.ncbi.nlm.nih.gov/orffinder/>). According to the search results, there existed no ORF more than 250 nt, and no proteins highly homologous to these oligopeptides possibly coded by the sense strands were found through smart BLAST search. It indicated that TCONS_00075467 could not be translated into protein. TCONS_00075467 was down-regulated in AF group (Fig. 3C). The coexpression network of TCONS_00075467 was associated with calcium signaling pathway (ko04020), MAPK signaling pathway (ko04010), arrhythmogenic right ventricular cardiomyopathy (ko05412), hypertrophic cardiomyopathy (ko05410), and dilated cardiomyopathy (ko05414) (Fig. 2C). These findings promoted us to focus on exploring the role of TCONS_00075467 in electrical remodeling during AF.

3.8 Biological effects of TCONS_00075467 in AF

3.8.1 Inhibition of TCONS_00075467 shortened AERP in vivo

To explore the knockdown efficiency of siRNA for TCONS_00075467, we stably inhibited TCONS_00075467 in primary cardiomyocytes. Then the lentiviruses containing four siRNAs in one shRNA were constructed and transfected into the RA to further investigate whether the lncRNA affect electrical remodeling. After 7 d infection, qRT-PCR analyses revealed that the targeting lentiviruses could remarkably reduce the expression of TCONS_00075467 compared with that of the negative control (Fig. 4A). Then electrophysiological parameters of the experimental and control groups were compared to examine its biological roles in AF initiation. The

AERP of RA did not reach statistical significance before and immediately after infection (Fig. 4C). However, after 7 d infection, inhibition of TCONS_00075467 expression could significantly shorten AERP (76 ± 8.2 vs. 102 ± 8.4 , $p < 0.01$) (Fig. 4C). AF was induced in three out of five rabbits, and paroxysmal atrial tachycardia (lasting < 30 s) existed in all five animals in the lenti-RNAi-TCONS_00075467 group, while in control group paroxysmal atrial tachycardia was induced in two rabbits (Fig. 4D). These differential ratios suggested that the down-regulation of TCONS_00075467 could increase the inducibility of AF.

3.8.2 TCONS_00075467 was physically associated with miR-328 in cardiomyocytes

According to the cis- and trans- prediction for TCONS_00075467, no target genes were found associated with atrial electrical remodeling or ion channels in AF. Therefore TCONS_00075467 may exert biological effects through other mechanisms. Recently, several studies indicated that lncRNA may operate as a competing endogenous RNA (ceRNA) in pathogenesis of heart disease [36]. The hypothesis of ceRNA function supposes that some specific lncRNAs can function as miRNA sponges to control miRNAs available for binding with their targets, functionally liberating their target mRNA transcripts [37]. Based on the bioinformatics analysis, we speculated that TCONS_00075467 may interact with miR-328. Given that miRNAs mainly exert their functions in cytoplasm, we performed *in situ* hybridization to confirm the existence of TCONS_00075467 in cytoplasm. As shown in Figure 3E, TCONS_00075467 was found to be mostly localized in the cytoplasm of primary myocytes. Previous studies supported an important role for miR-328 in AF [31]. Consistently, we found that miR-328 was up-regulated significantly in AF model (Fig. 3C). In contrast, the *in vivo* experiment verified the antagonistic effect of TCONS_00075467 on electrical remodeling in AF (Fig.1B).

To further explore the connection between TCONS_00075467 and miR-328, bivariate correlation analysis was made and results showed that expression of TCONS_00075467 was negatively correlated with miR-328 transcript level in RA of AF model (Fig. 3D). After gene interference experiments, qRT-PCR showed that endogenous TCONS_00075467 was reduced in lenti-miR-328 mimics infected cells, and lenti-miR-328 inhibitor increased TCONS_00075467 levels (Fig. 5C). Whereas down-regulation of TCONS_00075467 could up-regulate the expression of miR-328 in primary cardiomyocytes and RA (Fig. 5D). These data further verified that TCONS_00075467 was negatively correlated with miR-328 in cardiomyocytes. Four potential binding sites of miR-328 in TCONS_00075467 were identified by bioinformatics analysis (Fig. 5A). To detect the interaction between TCONS_00075467 and miR-328, luciferase assay was performed. The fragments containing binding sites and their mutations were cloned to psiCkeck2 vector respectively, named psi-TCONS_00075467-WT and psi-TCONS_00075467-Mut. After co-transfection with psi-TCONS_00075467-WT and miR-328 mimics, there was an obvious decrease in luciferase activity compared with the negative control in HEK293T cells (Fig. 5B). However, co-transfection with psi-TCONS_00075467-Mut and miR-328 mimics showed no effects on the luciferase reporter activities (Fig. 5B).

3.8.3 MiR-328 induced electrical remodeling in AF model

The miR-328 mimics and miR-328 inhibitor lentiviruses were infected into RA to further study the function of miR-328 (Fig. 4B). After 7 d infection, compared with

the negative control group, AERP significantly decreased in the lenti-miR-328 mimics group (70 ± 7.9 vs. 98 ± 6.7 , $p < 0.01$), while AERP markedly increased in the lenti-miR-328 inhibitor group (118 ± 5.7 vs. 99 ± 7.4 , $p < 0.01$) (Fig. 4C). Compared with the control group in which paroxysmal atrial tachycardia (lasting <30 s) was induced in two rabbits, AF was induced in four out of five animals, and paroxysmal atrial tachycardia existed in all five animals in the lenti-miR-328 mimics group. By contrast, no paroxysmal atrial tachycardia and AF were observed in the lenti-miR-328 inhibitor group (Fig. 4D).

3.8.4 MiR-328 targeted and negatively regulated CACNA1C

From the TargetScan database and previous studies [31], we found the binding sites of miR-328 that matched to the 3'UTR of CACNA1C, which suggested that CACNA1C was the potential target of miR-328 (Fig. 5E). Subsequently, the luciferase reporter vectors containing the wild-type (psi-CACNA1C-WT) and mutant (psi-CACNA1C-Mut) binding sites were generated. The luciferase reporter assays showed that co-infection with miR-328 mimics and psi-CACNA1C-WT led to a marked decrease in luciferase activity, while the luciferase activity of co-infection with miR-328 mimics and psi-CACNA1C-Mut without significant change compared with negative group (Fig. 5F).

To determine whether miR-328 regulated the CACNA1C, we detected the expression of CACNA1C after changing the expression of miR-328 in primary myocytes and RA. These results demonstrated that the up-regulation of miR-328 led to a decrease in CACNA1C protein expression, while inhibition of miR-328 induced an increase in CACNA1C protein expression (Fig. 6A). We then further ruled out the possibility that miR-328 acts by targeting ion channels other than CACNA1C (Fig. A.4).

3.8.5 TCONS-00075467 down regulated CACNA1C expression as ceRNA

The expression level of CACNA1C was inhibited both in cardiomyocytes and RA after infection with RNAi-TCONS_00075467 lentiviruses compared with the negative control group by Western Blot (Fig. 6B). As depicted in Figure 6E, I_{CaL} density of primary myocytes after infection with RNAi-TCONS_00075467 lentiviruses was substantially decreased (Fig. 6F), atrial APD was markedly shortened (Fig. 6C), and rate accommodation of APD was abolished (Fig. 6D), which were similar to feature of atrial electrical remodeling seen in experimental and clinical AF [29, 38].

To further establish a functional connection between miR-328 and TCONS_00075467, we tested whether TCONS_00075467 deregulation was required for regulation of miR-328 on electrical remodeling. We transfected both miR-328 inhibitor lentiviruses or negative control and RNAi-TCONS_00075467 lentiviruses simultaneously to primary cardiomyocytes and RA *in vitro* and *in vivo* respectively. *In vivo* experiments, compared with lenti-RNAi-TCONS_00075467 group, AERP increased markedly in co-infection with RNAi-TCONS_00075467 and miR-328 inhibitor lentiviruses group (106 ± 9.6 vs. 76 ± 8.2 , $p < 0.01$), but without significant difference compared with negative control group (106 ± 9.6 vs. 97 ± 7.6) (Fig. 4C). As mentioned above, AF was induced in three out of five rabbits, and paroxysmal atrial tachycardia (lasting <30 s) existed in all five animals in the lenti-RNAi-TCONS_00075467 group, while paroxysmal atrial tachycardia was induced in three out of five rabbits, and no AF induction was observed in the co-infection with RNAi-

TCONS_00075467 and miR-328 inhibitor lentiviruses group (Fig. 4D). Western Blot showed that RNAi-TCONS_00075467 could inhibit the expression of CACNA1C whereas miR-328 inhibitor could relieve the inhibition of CACNA1C by TCONS_00075467 (Fig. 6B).

Taken together, these data indicate that by binding miR-328, TCONS_00075467 acts as a ceRNA for the target CACNA1C expression thereby imposing an repression on post-transcriptional regulation.

4. Discussion

At present, the routine therapies of internal medicine for AF include pharmacotherapy and radiofrequency ablation. The former is the basic therapy for AF patients with possible adverse effects and poor tolerance. The success ratio of radiofrequency ablation to cure AF has been greatly improved but it still exits high recurrence rate after ablation, especially in permanent AF patients. The less satisfactory therapeutic effects on AF should be closely related to its unclear pathogenesis mechanisms. So the innovative research on the molecular mechanisms of AF is needed. In this study, the main findings were as follows: (I) the right atrial electrical remodeling plays an important role in the initiation of AF; (II) the altered expression profile of lncRNAs in RA of rabbit AF models was confirmed using high-throughput RNA-Seq; (III) according to bioinformatic analyses, the lncRNA (TCONS_00075467) related to electrical remodeling during AF was identified, and knockdown of TCONS_00075467 in RA induced AERP shortened and AF inducibility increased significantly; (IV) TCONS_00075467 could modulate atrial electrical remodeling by sponging miR-328 as a ceRNA to regulate CACNA1C expression.

The electrical remodeling emerges in RA accompanying with AF. Many studies had verified that electrical remodeling, such as the significant changes of potassium and calcium currents and APD shortened, occurred in RA of patients with AF and canine AF models by right atrial rapid pacing [29, 30]. Recently Li N *et al* proved that the high expression level of adenosine A1 receptor and GIRK4 in RA showed higher inducibility of AF [39]. Our previous studies also proved that miR-1 promoted the electrical remodeling in RA, and shortened the AERP, which facilitated the initiation of AF [18]. So the right atrial electrical remodeling also plays important role in the initiation and maintenance of AF. Several reports have demonstrated that right atrial ablation increases the success rate of maintaining sinus rhythm in certain patients with AF [40, 41]. The study on right atrial electrical remodeling may provide a new therapeutic target for AF.

LncRNAs, although initially considered as genomic transcription noise, have been demonstrated to play pivotal roles in multiple biological processes and are increasingly recognized as contributors to the pathogenesis of ventricular septal defects [42], myocardial infarction [43], heart failure [44], and cardiac hypotrophy [13]. As to AF, the expression patterns of lncRNAs in human atria and serum were reported in two papers [15, 45]. However they only referred that the lncRNAs were closely related to the pathogenesis of AF, the regulatory roles and exact mechanisms of lncRNAs in the pathogenesis of AF remain unclear. So we build the rabbit AF models with atrial tachypacing to identify the lncRNAs related to electrical

remodeling and further investigate the functions and mechanisms of the lncRNAs in RA.

In our study, a total of 99843 putative new lncRNAs were detected by the high-throughput RNA-Seq, and up to 1220 lncRNAs were expressed with more than 2-fold change, which had not been functionally characterized. These findings indicate that lncRNAs display a unique expression profile in AF. Compared with studies on miRNAs, those on lncRNAs are not yet comprehensive. Only few bioinformatic means can be used to predict the functions and mechanisms of lncRNAs interfering in the co-expressed protein-coding genes. GO functional analysis is widely used to illustrate the differentially expressed genes in terms of biological roles and molecular functions. In this study, the main biological processes representing dysregulated lncRNAs were closely associated with transmembrane ion transport and extracellular matrix remodeling, including “calcium ion binding,” “transmembrane transport,” “extracellular matrix organization,” and “cell adhesion.” Similarly, KEGG pathway analysis concluded that the differentially expressed genes mainly belonged to the pathways involved in calcium signaling pathway, arrhythmia and cardiomyopathy disorders. Our bioinformatic results were similar to those of lncRNAs profiles in AF patients [15, 45], but the rabbit models facilitated us to conduct the functional verification of the aberrantly expressed lncRNAs *in vivo* and *in vitro*.

Though bioinformatics analysis showed that the specific expressed genes were closely associated with atrial remodeling, the selection of lncRNAs related to AF atrial remodeling can not be merely based on GO and KEGG pathway analyses. Besides, considering that the relationships between the poorly conserved sequence or secondary structure of lncRNAs and their functions are still unclear, the functions of lncRNAs are difficult to elucidate by their nucleotide sequence directly [46]. Therefore, a series of filtering approaches were adopted to identify candidate lncRNAs. Firstly, transcripts with significant expression changes were selected to exclude the nonsense transcripts from sequencing errors. Then the biological roles of their target genes were elucidated by bioinformatics analysis in order to interpret the functions of lncRNAs. Subsequently the relative expression abundance and conserved sequence matched to human genome were also considered. Given that lncRNAs spatially and temporally expressed in some tissues [42], nervous tissue, aorta, skeletal muscle and atrial tissue were detected. Thus the transcripts only highly expressed in atrial tissue were selected. Finally, TCONS_00075467 were confirmed that may play a role in electrical remodeling.

To investigate the potential involvement of the novel lncRNA in AF electrical remodeling, loss-of-function experiments were conducted. There was no significant difference of AERP before and immediately after infection between the groups, which suggested that the operation of infection did not contribute to the electrophysiological changes. However, after 7 d infection, inhibition of TCONS_00075467 in RA induced AERP shortened and AF inducibility increased significantly, which implied AF vulnerability increased [47]. In summary, these findings indicate that TCONS_00075467 could suppress the occurrence of electrical remodeling and the initiation of AF.

Although this lncRNA exerted important biological effects on shortening of AERP, the molecular mechanisms by which it modulated the process remain unknown. Previous studies show that lncRNAs, especially lincRNAs, may act in cis to regulate

the expression of neighboring protein-coding genes [48]. For example, TCONS_00032546 could modulate its nearby gene FGF19 expression by cis-mechanism to contribute the autonomic neural remodeling of AF in canine model [17]. Considering that TCONS_00075467 belongs to lincRNAs, the nearby genes should be investigated after loss-of-function experiment. But the location of TCONS_00075467 is distant from the 3 kilobase upstream or downstream sequences (transcriptional start sites) of the known protein-coding transcripts and the nearby genes have little relation with initiation of AF. Meanwhile, no meaningful target genes were found through trans-prediction. Thus TCONS_00075467 may not exert biological effects by cis- or trans-mechanism. Recently, accumulating evidence reveals that many lincRNAs, such as MALAT1 and HOTAIR, which are classical examples of lincRNAs, act as ceRNA to regulate the protein expression of target genes [12, 49]. With regard to myocardium, the lincRNA, cardiac hypertrophy-related factor, was able to down-regulate miR-489 expression levels and regulate Myd88 expression in hypertrophy [50]. It is possible that there may exist some miRNAs interact with TCONS_00075467 to modulate the electrical remodeling in AF. So the interacting miRNAs of TCONS_00075467 should be further investigated in the pathogenesis of AF.

CeRNAs are endogenous transcripts that, irrespectively of their ability to encode for a protein, share common miRNA Recognition Elements and hence compete for the binding of usual miRNA molecules. The outcome of such competition is that ceRNAs relieve each other from miRNA-mediated inhibition and positively impact each other's expression levels [51]. And the abundant expression and location in cytoplasm of TCONS_00075467 provides a possible condition for ceRNA function.

According to the bioinformatics analysis, miR-328 was selected to be co-acted with the lincRNA. Previous studies had confirmed that miR-328 contributed to the AF remodeling and cardiac hypertrophy [31, 52], but the new mechanisms of miR-328 were investigated in electrical remodeling during AF in this study. We first examined the expression of TCONS_00075467 and miR-328 in 12 AF and non-AF rabbit models and genes interference experiments. We found that TCONS_00075467 was down regulated in AF group while miR-328 existed higher fold change (AF/non-AF). Bivariate correlation analysis showed that expression of TCONS_00075467 was negatively correlated with miR-328 transcript level. We then found that knockdown of TCONS_00075467 could up-regulate miR-328 level. Meanwhile silencing miR-328 could up-regulate TCONS_00075467 level and the expression of TCONS_00075467 was widely decreased after infection with miR-328 mimics. We employed bioinformatics analysis and found that TCONS_00075467 may exist four binding sites for miR-328. Then the luciferase reporter assay indicated that TCONS_00075467 could strongly combine with miR-328. As mentioned above, the interaction between TCONS_00075467 and miR-328 may exert biological effects through intervening in the expression of CACNA1C ultimately. Calcium voltage-gated channel subunit alpha1 C, CACNA1C briefly, encodes an alpha-1 subunit of a voltage-dependent calcium channel. The alpha-1 subunit forms the L-type calcium channel, Cav1.2, through which calcium ions pass into the cell. Alterations of calcium channels are the mainly changes of ion channels in AF, and previous studies confirmed that CACNA1C was down-regulated in patients with AF and rheumatic heart disease and in a canine model of AF [31]. Furthermore, a genetic research in familial AF suggested that rare variants of Cav1.2 could identify an important pathway modulating AF susceptibility [53]. The decreased expression of CACNA1C

could induce intracellular calcium overload, which is the main mechanism of initiation and maintenance of AF. The CACNA1C expression affected by miRNAs had been reported [31, 54], but the roles of lncRNA in this alteration had not been referred. MiR-328 up-regulation led to a decrease in CACNA1C protein expression, while inhibition of miR-328 induced an increase in CACNA1C protein expression. We found that knockdown of TCONS_00075467 could inhibit the expression of CACNA1C by Western Blot, decrease I_{CaL} density and shorten APD by patch-clamp. After CACNA1C silencing, the mRNAs of downstream pathway related to CACNA1C, such as CALM1, CALM2, CALML4, CAMK2A and RYR2 were up-regulated, suggesting an influence on calcium signaling pathway (Fig. A.5). And the luciferase reporter assay also showed that miR-328 could bind to the 3'UTR of CACNA1C mRNA. What's more, the co-infection experiments demonstrated that knockdown of TCONS_00075467 could decrease the expression of CACNA1C whereas miR-328 inhibitor could partly reverse the reduction caused by knockdown of TCONS_00075467. In summary, TCONS_00075467 was down-regulated while miR-328 exist generally higher expression in cardiomyocytes of AF. So the decreased abundance of TCONS_00075467 could modulate the expression of CACNA1C in cardiomyocytes of AF through miR-328 as a ceRNA.

Though the novel lncRNA was demonstrated to play distinct roles in electrical remodeling during AF, there are few limitations in this study. It can't be assumed that the rabbit model of AF after right atrial rapid pacing is directly analogous to clinical AF. The left atrial pacing was not conducted in this study. The mechanism underlying modification of lncRNAs by atrial tachycardia will be examined in the next work.

5. Conclusion

This study illustrated the profiles of significantly expressed lncRNAs of RA in AF and non-AF rabbit models by using high-throughput RNA-Seq. The novel lncRNA TCONS_00075467 was demonstrated to have important biological effects on right atrial electrical remodeling during AF, which modulated the expression of CACNA1C by binding miR-328 as a ceRNA. The right atrial electrical remodeling played important roles in the initiation of AF. The results suggested a remarkable functional importance of lncRNAs in electrical remodeling during AF, thereby facilitating the mechanism studies of lncRNAs in AF pathogenesis and providing potential therapeutic targets for AF.

Acknowledgements

This work was supported by the National Natural Science Foundation of China (81270237), Lisheng Cardiovascular Health Foundation (LHJJ20159423) and Taishan Scholar Engineering Construction Fund of Shandong Province.

Conflict of Interest Disclosures: None.

References

- [1] Thomas IC, Sorrentino MJ. Bleeding risk prediction models in atrial fibrillation. *Curr Cardiol Rep* 2014; 16: 432.

- [2] Conen D, Chae CU, Glynn RJ, Tedrow UB, Everett BM, Buring JE, et al. Risk of death and cardiovascular events in initially healthy women with new-onset atrial fibrillation. *JAMA* 2011; 305: 2080-7.
- [3] Brundel BJ, Van Gelder IC, Henning RH, Tuinenburg AE, Wietses M, Grandjean JG, et al. Alterations in potassium channel gene expression in atria of patients with persistent and paroxysmal atrial fibrillation: differential regulation of protein and mRNA levels for K⁺ channels. *J Am Coll Cardiol* 2001; 37: 926-32.
- [4] Allessie M, Ausma J, Schotten U. Electrical, contractile and structural remodeling during atrial fibrillation. *Cardiovasc Res* 2002; 54: 230-46.
- [5] Xie W, Santulli G, Guo X, Gao M, Chen BX, Marks AR. Imaging atrial arrhythmic intracellular calcium in intact heart. *J Mol Cell Cardiol* 2013; 64: 120-3.
- [6] Krogh-Madsen T, Abbott GW, Christini DJ. Effects of electrical and structural remodeling on atrial fibrillation maintenance: a simulation study. *PLoS Comput Biol* 2012; 8: e1002390.
- [7] Cha TJ, Ehrlich JR, Zhang L, Chartier D, Leung TK, Nattel S. Atrial tachycardia remodeling of pulmonary vein cardiomyocytes: comparison with left atrium and potential relation to arrhythmogenesis. *Circulation* 2005; 111: 728-35.
- [8] den Hoed M, Eijgelsheim M, Esko T, Brundel BJ, Peal DS, Evans DM, et al. Identification of heart rate-associated loci and their effects on cardiac conduction and rhythm disorders. *Nat Genet* 2013; 45: 621-31.
- [9] Santulli G, Iaccarino G, De Luca N, Trimarco B, Condorelli G. Atrial fibrillation and microRNAs. *Front Physiol* 2014; 5: 15.
- [10] Saxena A, Carninci P. Long non-coding RNA modifies chromatin: epigenetic silencing by long non-coding RNAs. *Bioessays* 2011; 33: 830-9.
- [11] Niland CN, Merry CR, Khalil AM. Emerging Roles for Long Non-Coding RNAs in Cancer and Neurological Disorders. *Front Genet* 2012; 3: 25.
- [12] Xiao H, Tang K, Liu P, Chen K, Hu J, Zeng J, et al. LncRNA MALAT1 functions as a competing endogenous RNA to regulate ZEB2 expression by sponging miR-200s in clear cell kidney carcinoma. *Oncotarget* 2015; 6: 38005-15.
- [13] Han P, Li W, Lin CH, Yang J, Shang C, Nurnberg ST, et al. A long noncoding RNA protects the heart from pathological hypertrophy. *Nature* 2014; 514: 102-6.
- [14] Papait R, Kunderfranco P, Stirparo GG, Latronico MV, Condorelli G. Long noncoding RNA: a new player of heart failure? *J Cardiovasc Transl Res* 2013; 6: 876-83.
- [15] Xu Y, Huang R, Gu J, Jiang W. Identification of long non-coding RNAs as novel biomarker and potential therapeutic target for atrial fibrillation in old adults. *Oncotarget* 2016; 7: 10803-11.
- [16] Gore-Panter SR, Hsu J, Barnard J, Moravec CS, Van Wagoner DR, Chung MK, et al. PANCR, the PITX2 Adjacent Noncoding RNA, Is Expressed in Human Left Atria and Regulates PITX2c Expression. *Circ Arrhythm Electrophysiol* 2016; 9: e003197.
- [17] Wang W, Wang X, Zhang Y, Li Z, Xie X, Wang J, et al. Transcriptome analysis of canine cardiac fat pads: involvement of two novel long non-coding RNAs in atrial fibrillation neural remodeling. *J Cell Biochem* 2015; 116: 809-21.
- [18] Jia X, Zheng S, Xie X, Zhang Y, Wang W, Wang Z, et al. MicroRNA-1 accelerates the shortening of atrial effective refractory period by regulating KCNE1 and KCNB2 expression: an atrial tachypacing rabbit model. *PLoS One* 2013; 8: e85639.
- [19] Rohrbach S, Muller-Werdan U, Werdan K, Koch S, Gellerich NF, Holtz J. Apoptosis-modulating interaction of the neuregulin/erbB pathway with anthracyclines

- in regulating Bcl-xS and Bcl-xL in cardiomyocytes. *J Mol Cell Cardiol* 2005; 38: 485-93.
- [20] Trapnell C, Pachter L, Salzberg SL. TopHat: discovering splice junctions with RNA-Seq. *Bioinformatics* 2009; 25: 1105-11.
- [21] Shannon P, Markiel A, Ozier O, Baliga NS, Wang JT, Ramage D, et al. Cytoscape: a software environment for integrated models of biomolecular interaction networks. *Genome Res* 2003; 13: 2498-504.
- [22] Milo R, Shen-Orr S, Itzkovitz S, Kashtan N, Chklovskii D, Alon U. Network motifs: simple building blocks of complex networks. *Science* 2002; 298: 824-7.
- [23] Liu Z, Zhou C, Liu Y, Wang S, Ye P, Miao X, et al. The expression levels of plasma microRNAs in atrial fibrillation patients. *PLoS One* 2012; 7: e44906.
- [24] Shi KH, Tao H, Yang JJ, Wu JX, Xu SS, Zhan HY. Role of microRNAs in atrial fibrillation: new insights and perspectives. *Cell Signal* 2013; 25: 2079-84.
- [25] Lu Y, Hou S, Huang D, Luo X, Zhang J, Chen J, et al. Expression profile analysis of circulating microRNAs and their effects on ion channels in Chinese atrial fibrillation patients. *Int J Clin Exp Med* 2015; 8: 845-53.
- [26] Wang J, Song S, Xie C, Han J, Li Y, Shi J, et al. MicroRNA profiling in the left atrium in patients with non-valvular paroxysmal atrial fibrillation. *BMC Cardiovasc Disord* 2015; 15: 97.
- [27] Wang T, Wang B. Identification of microRNA-mRNA interactions in atrial fibrillation using microarray expression profiles and bioinformatics analysis. *Mol Med Rep* 2016; 13: 4535-40.
- [28] Yang B, Lin H, Xiao J, Lu Y, Luo X, Li B, et al. The muscle-specific microRNA miR-1 regulates cardiac arrhythmogenic potential by targeting GJA1 and KCNJ2. *Nat Med* 2007; 13: 486-91.
- [29] Yue L, Feng J, Gaspo R, Li GR, Wang Z, Nattel S. Ionic remodeling underlying action potential changes in a canine model of atrial fibrillation. *Circ Res* 1997; 81: 512-25.
- [30] Bosch RF, Zeng X, Grammer JB, Popovic K, Mewis C, Kuhlkamp V. Ionic mechanisms of electrical remodeling in human atrial fibrillation. *Cardiovasc Res* 1999; 44: 121-31.
- [31] Lu Y, Zhang Y, Wang N, Pan Z, Gao X, Zhang F, et al. MicroRNA-328 contributes to adverse electrical remodeling in atrial fibrillation. *Circulation* 2010; 122: 2378-87.
- [32] Leucci E, Patella F, Waage J, Holmstrom K, Lindow M, Porse B, et al. microRNA-9 targets the long non-coding RNA MALAT1 for degradation in the nucleus. *Sci Rep* 2013; 3: 2535.
- [33] Climent AM, Guillem MS, Fuentes L, Lee P, Bollensdorff C, Fernandez-Santos ME, et al. Role of atrial tissue remodeling on rotor dynamics: an in vitro study. *Am J Physiol Heart Circ Physiol* 2015; 309: H1964-73.
- [34] Zhang Y, Dong D, Yang B. Atrial remodeling in atrial fibrillation and association between microRNA network and atrial fibrillation. *Sci China Life Sci* 2011; 54: 1097-102.
- [35] Clark BS, Blackshaw S. Long non-coding RNA-dependent transcriptional regulation in neuronal development and disease. *Front Genet* 2014; 5: 164.
- [36] Song C, Zhang J, Liu Y, Pan H, Qi HP, Cao YG, et al. Construction and analysis of cardiac hypertrophy-associated lncRNA-mRNA network based on competitive endogenous RNA reveal functional lncRNAs in cardiac hypertrophy. *Oncotarget* 2016; 7: 10827-40.

- [37] Arancio W, Pizzolanti G, Genovese SI, Baiamonte C, Giordano C. Competing endogenous RNA and interactome bioinformatic analyses on human telomerase. *Rejuvenation Res* 2014; 17: 161-7.
- [38] Nattel S. Atrial electrophysiological remodeling caused by rapid atrial activation: underlying mechanisms and clinical relevance to atrial fibrillation. *Cardiovasc Res* 1999; 42: 298-308.
- [39] Li N, Csepe TA, Hansen BJ, Sul LV, Kalyanasundaram A, Zakharkin SO, et al. Adenosine-Induced Atrial Fibrillation: Localized Reentrant Drivers in Lateral Right Atria due to Heterogeneous Expression of Adenosine A1 Receptors and GIRK4 Subunits in the Human Heart. *Circulation* 2016; 134: 486-98.
- [40] Lin YJ, Tai CT, Kao T, Tso HW, Huang JL, Higa S, et al. Electrophysiological characteristics and catheter ablation in patients with paroxysmal right atrial fibrillation. *Circulation* 2005; 112: 1692-700.
- [41] Hocini M, Nault I, Wright M, Veenhuyzen G, Narayan SM, Jais P, et al. Disparate evolution of right and left atrial rate during ablation of long-lasting persistent atrial fibrillation. *J Am Coll Cardiol* 2010; 55: 1007-16.
- [42] Song G, Shen Y, Zhu J, Liu H, Liu M, Shen YQ, et al. Integrated analysis of dysregulated lncRNA expression in fetal cardiac tissues with ventricular septal defect. *PLoS One* 2013; 8: e77492.
- [43] Ishii N, Ozaki K, Sato H, Mizuno H, Saito S, Takahashi A, et al. Identification of a novel non-coding RNA, MIAT, that confers risk of myocardial infarction. *J Hum Genet* 2006; 51: 1087-99.
- [44] Zhu JG, Shen YH, Liu HL, Liu M, Shen YQ, Kong XQ, et al. Long noncoding RNAs expression profile of the developing mouse heart. *J Cell Biochem* 2014; 115: 910-8.
- [45] Ruan Z, Sun X, Sheng H, Zhu L. Long non-coding RNA expression profile in atrial fibrillation. *Int J Clin Exp Pathol* 2015; 8: 8402-10.
- [46] Guo X, Gao L, Liao Q, Xiao H, Ma X, Yang X, et al. Long non-coding RNAs function annotation: a global prediction method based on bi-colored networks. *Nucleic Acids Res* 2013; 41: e35.
- [47] Linz D, Mahfoud F, Schotten U, Ukena C, Neuberger HR, Wirth K, et al. Effects of electrical stimulation of carotid baroreflex and renal denervation on atrial electrophysiology. *J Cardiovasc Electrophysiol* 2013; 24: 1028-33.
- [48] Ponjavic J, Oliver PL, Lunter G, Ponting CP. Genomic and transcriptional colocalization of protein-coding and long non-coding RNA pairs in the developing brain. *PLoS Genet* 2009; 5: e1000617.
- [49] Bian EB, Ma CC, He XJ, Wang C, Zong G, Wang HL, et al. Epigenetic modification of miR-141 regulates SKA2 by an endogenous 'sponge' HOTAIR in glioma. *Oncotarget* 2016; 7: 30610-25.
- [50] Wang K, Liu F, Zhou LY, Long B, Yuan SM, Wang Y, et al. The long noncoding RNA CHRF regulates cardiac hypertrophy by targeting miR-489. *Circ Res* 2014; 114: 1377-88.
- [51] Poliseno L, Salmena L, Zhang J, Carver B, Haveman WJ, Pandolfi PP. A coding-independent function of gene and pseudogene mRNAs regulates tumour biology. *Nature* 2010; 465: 1033-8.
- [52] Li C, Li X, Gao X, Zhang R, Zhang Y, Liang H, et al. MicroRNA-328 as a regulator of cardiac hypertrophy. *Int J Cardiol* 2014; 173: 268-76.
- [53] Weeke P, Muhammad R, Delaney JT, Shaffer C, Mosley JD, Blair M, et al. Whole-exome sequencing in familial atrial fibrillation. *Eur Heart J* 2014; 35: 2477-83.

[54] Barana A, Matamoros M, Dolz-Gaiton P, Perez-Hernandez M, Amoros I, Nunez M, et al. Chronic atrial fibrillation increases microRNA-21 in human atrial myocytes decreasing L-type calcium current. *Circ Arrhythm Electrophysiol* 2014; 7: 861-8.

ACCEPTED MANUSCRIPT

Figure Legends:

Figure 1: Characterization of AF in the rabbit model. (A) Electrocardiograph of the sinus rhythm and AF obtained. (B) The AERP of control group and AF group obtained in right atrium. (C) The AF inducibility obtained from control group and AF group. (D) The protein expression of key ion channels obtained in right atrium from control group and AF group. * $p < 0.05$ and ** $p < 0.01$.

Figure 2: Analysis of differentially expressed lncRNAs in RA of AF model. (A) Heat map of the new lncRNAs between control and AF groups. Expression levels are reflected by color change. Red indicates higher expression, whereas green indicates lower expression. TCONS_00075467 are marked with rectangle box. (B) The volcano plot of differentially expressed lncRNAs based on p -value and fold change. (C) The coexpression network obtained by Pearson's correlation coefficients. (D) GO analysis and (E) KEGG pathways analysis with the lowest p -value showed the biological processes that the significantly expressed lncRNAs may be involved in.

Figure 3: Identification of candidate lncRNAs in electrical remodeling. (A) Expression levels of six differentially expressed new lncRNAs were confirmed in AF/non-AF atria. (B) Expression levels of two candidate lncRNAs were compared in different tissues from rabbit. (C) Expression levels of TCONS_00075467 and its associated miR-328 were compared in AF/ non-AF atria. (D) The linear correlation analysis between TCONS_00075467 and its associated miR-328 in AF/ non-AF atria, atrial tissue and primary myocytes infected with lentiviruses respectively. (E) The colocalization of TCONS_00075467 and miR-328 in primary myocytes by RNA fluorescence *in situ* hybridization. TCONS_00075467 in red, miR-328 in green and DAPI is in blue. Magnification 400 \times . * $p < 0.05$ and ** $p < 0.01$.

Figure 4: Functions of TCONS_00075467 and miR-328. (A) Expression level of TCONS_00075467 was examined after 7 d infection in RA. (B) Expression level of miR-328 was examined after 7 d infection in RA. (C) The AERP was measured after infection in RA. (D) The AF inducibility was measured after 7 d infection in RA. * $p < 0.05$ and ** $p < 0.01$.

Figure 5: The interaction between TCONS_00075467 and miR-328, as well as between miR-328 and 3'UTR of CACNA1C. (A) The predicted binding sites between TCONS_00075467 and miR-328 obtained by bioinformatics analysis, and the mutation type of binding sites listed. (B) Luciferase reporters harboring putative target sites in the TCONS_00075467-WT or TCONS_00075467-Mut were co-transfected with miR-328 mimics in HEK293T cells. Relative luciferase activity was plotted as the mean \pm SEM of six independent experiments. (C) The relative expression of TCONS_00075467 was measured in primary myocytes and RA after infection with miR-328 inhibitor or mimics. (D) The relative expression of miR-328 was measured in primary myocytes and RA after infection with RNAi-TCONS_00075467. (E) The predicted binding site between miR-328 and 3'UTR of CACNA1C obtained by bioinformatics analysis, and the mutation type of binding site listed. (F) Luciferase reporters harboring putative target site in the 3'UTR of CACNA1C-WT or CACNA1C-Mut were co-transfected with miR-328 mimics in HEK293T cells. * $P < 0.05$ and ** $P < 0.01$.

Figure 6: The effects of TCONS_00075467 and miR-328 on CACNA1C. (A) The expression of CACNA1C was measured in primary myocytes and RA after infection with miR-328 inhibitor or mimics by western blot. (B) The expression of CACNA1C was measured in primary myocytes and RA after infection with RNAi-TCONS_00075467 and miR-328 inhibitor by western blot. (C) The action potential recording and (D) rate-adaption of action potential duration to 90% repolarization (APD_{90}) were obtained from primary myocytes infected with negative or RNAi-TCONS_00075467 lentiviruses (n=10) *in vitro*. (E) and (F) The I_{CaL} density were obtained from primary myocytes infected with negative or RNAi-TCONS_00075467 lentiviruses (n=10) *in vitro*. * $p < 0.05$ and ** $p < 0.01$.

Appendix Figure A.1: Characterization of AF in left atrium of rabbit model. (A) The protein expression of key ion channels obtained in left atrium from control group and AF group. (B) The AERP of control group and AF group obtained in left atrium. * $p < 0.05$ and ** $p < 0.01$.

Appendix Figure A.2: The distribution of the total mapped reads onto the genome obtained.

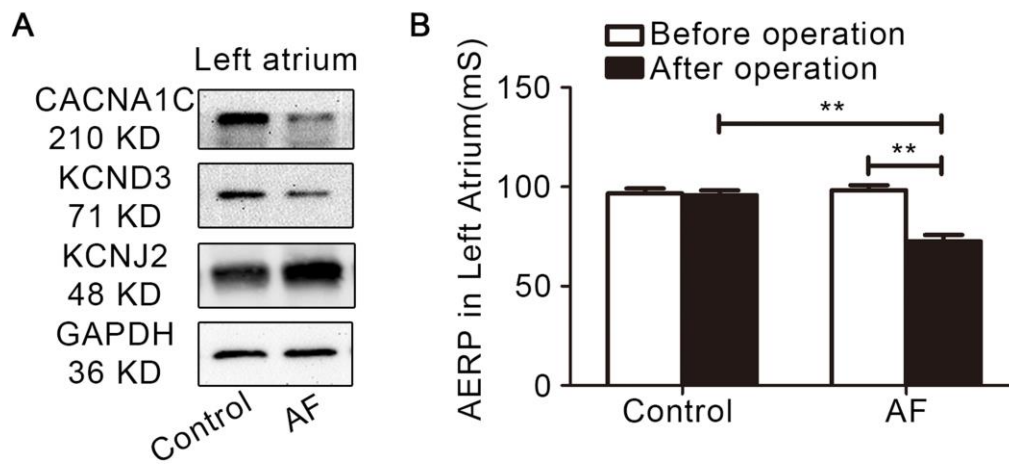
Appendix Figure A.3: The conserved transcript of TCONS_00075467 was obtained in human atria. (A) The conserved transcript of TCONS_00075467 obtained in human atria compared to rabbit atria. (B) The relative expression of conserved transcript of TCONS_00075467 were compared in human atria with AF/non-AF. * $p < 0.05$.

Appendix Figure A.4: The expression level of KCNJ2 and KCND3 were compared in RA after infection with lentiviruses by western blot.

Appendix Figure A.5: The relative expression of downstream pathway related to CACNA1C obtained from primary myocytes after CACNA1C silencing. * $p < 0.05$.

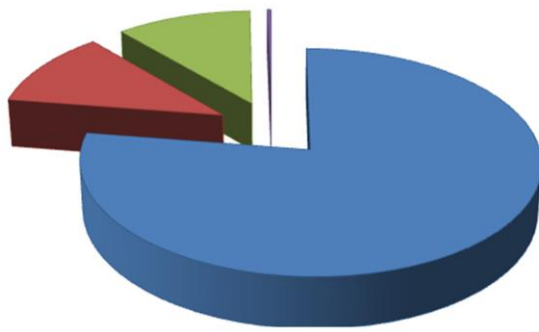
Appendix Figure A.6: The relative expression of differentially expressed lncRNAs in left atrium of AF model. * $p < 0.05$ and ** $p < 0.01$.

Appendix Figure A.1



ACCEPTED MANUSCRIPT

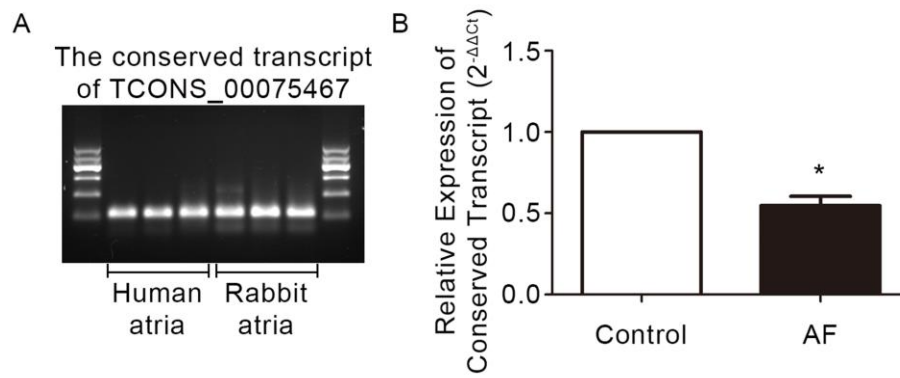
Appendix Figure A.2



■ exonic	77.4%
■ intronic	11.3%
■ intergenic	11.0%
■ splicing	0.3%

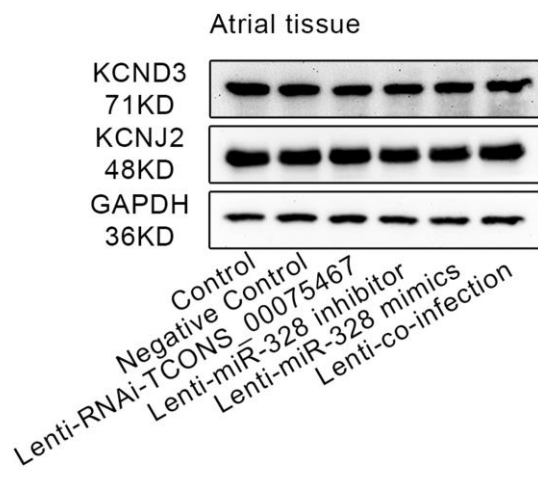
ACCEPTED MANUSCRIPT

Appendix Figure A.3



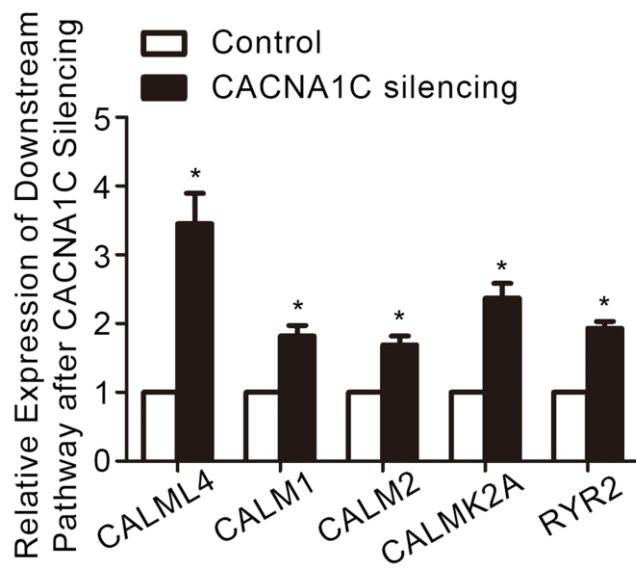
ACCEPTED MANUSCRIPT

Appendix Figure A.4



ACCEPTED MANUSCRIPT

Appendix Figure A.5



Appendix Figure A.6

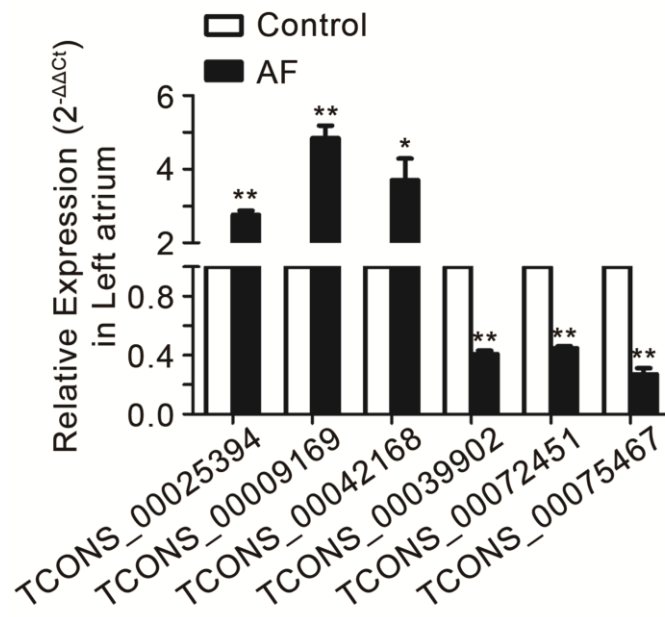


Table A.1 Primer Sequence

Gene Name	Primer Sequences
GAPDH	Forward: 5'- ACTTCGGCATTGTGGAGG -3' Reverse: 5'- GGAGGCAGGGATGATGTTCT -3'
TCONS_00075467	Forward: 5'- CCAGGCAAATGGGAGCACA -3' Reverse: 5'- CTTCCAGGCAACAACACTGA -3'
CACNA1C	Forward: 5'- ACTCCCACACGGAAGACAAG -3' Reverse: 5'- GACGAAACCCACGAAGATGT -3'
TCONS_00074073	Forward: 5'- TGTTTGAGCAC AAGACCCGA -3' Reverse: 5'- CCTGGAAGGGTTTGCAGTCT -3'
TCONS_00042168	Forward: 5'- CAATGTTGGTTGTCTGCATGT -3' Reverse: 5'- GGAAAGAATGCCTGGGTGT -3'
TCONS_00009169	Forward: 5'- GTCTTTGCTTTGTCATCAGTT -3' Reverse: 5'- CTTTTCATAGGCATTTAGGG -3'
TCONS_00025394	Forward: 5'- GTGTGGTTAAAGGTTGCCGC -3' Reverse: 5'- GGCCAAGGGGTCATGCTATT -3'
TCONS_00072451	Forward: 5'- CTAATGGGAACCGTGTCTGG -3' Reverse: 5'- ATGCCCTTGTCTTTGCTCTG -3'
TCONS_00039902	Forward: 5'- GGATAGTAAGAGAGATTGCGAGGA -3' Reverse: 5'- GGAGCAGCCAGGATTTGAT -3'
TCONS_00053509	Forward: 5'- CACATCCCACATCAGAATGC -3' Reverse: 5'- CAGGAGCCAGGAACTCAATC -3'
U6	Forward: 5'- CTCGCTTCGGCAGCACA -3'
miR-328	Forward: 5'- CGGCTGGCCCTCTCTGCCCTTCCG -3'

Table A.2 siRNA and Mimics Sequences

Name	Sequences(5' to 3')
TCONS_00075467 siRNA613	Sense: CCUCCCAGAGGAGUAACUU Antisense: AAGUUACUCCUCUGGGAGG
TCONS_00075467 siRNA989	Sense: CCAGAU AAGGUGGCAGUUU Antisense: AACUGCCACCUUAUCUGG
TCONS_00075467 siRNA1260	Sense: GGUGCAGUGUGAGUAGCAA Antisense: UUGCUACUCACACUGCACC
TCONS_00075467 siRNA1385	Sense: GCCUCAGUAUUGAGGUC AA Antisense: UUGACCUCAAUACUGAGGC
Negative Control	Sense: UUCUCCGAACGUGUCACGU Antisense: ACGUGACACGUUCGGAGAA
miR-328 inhibitor	Sense: ACGGAAGGGCAGAGAGGGCCAG
miR-328 mimics	Sense: CUGGCCUUCUCUGCCCUUCCGU

Table A.3 Mapping Results Count

Sample name	sample 1	sample 2	sample 3
Total reads	57,669,122(100%)	71,188,754(100%)	70,345,416(100%)
Total mapped	50,137,237(86.94%)	60,974,200(85.65%)	61,814,239(87.87%)
Multiple mapped	3,166,210(5.49%)	4,526,960(6.36%)	4,692,114(6.67%)
Uniquely mapped	46,971,027(81.45%)	56,447,240(79.29%)	57,122,125(81.20%)
Read1 mapped	25,110,407(43.54%)	30,535,502(42.89%)	30,955,720(44.01%)
Read2 mapped	25,026,830(43.40%)	30,438,698(42.76%)	30,858,519(43.87%)
Reads mapped in proper pairs	24,010,189(41.63%)	29,334,020(41.21%)	29,750,217(42.29%)

Sample name	sample 4	sample 5	sample 6
Total reads	71,831,132(100%)	51,415,730(100%)	60,216,802(100%)
Total mapped	63,928,550(89.00%)	47,107,094(91.62%)	53,007,407(88.03%)
Multiple mapped	6,652,164(9.26%)	5,431,909(10.56%)	5,308,027(8.81%)
Uniquely mapped	57,276,386(79.74%)	41,675,185(81.06%)	47,699,380(79.21%)
Read1 mapped	31,988,524(44.53%)	23,574,020(45.85%)	26,526,749(44.05%)
Read2 mapped	31,940,026(44.47%)	23,533,074(45.77%)	26,480,658(43.98%)
Reads mapped in proper pairs	30,996,545(43.15%)	22,871,936(44.48%)	25,656,465(42.61%)

Table A.4 The composition of Tyrode and peptide solution

Current	Action potentials	I_{CaL}
Tyrode solution (mM)	NaCl 136, KCl 5.4, CaCl ₂ 2.0, MgCl ₂ 1.0, NaH ₂ PO ₄ 0.33, HEPES 5, Glucose 10 (pH 7.4 with NaOH)	CholineCl 136, CsCl 5.4, CaCl ₂ 2.0, MgCl ₂ 0.8, NaH ₂ PO ₄ 0.33, HEPES 5, Glucose 10 (pH 7.4 with CsOH)
Peptide solution (mM)	KCl 20, K-aspartate 110, MgCl ₂ 1.0, HEPES 10, EGTA 5, Mg ₂ ATP 5, GTP 0.1, phosphocreatine 5 (pH 7.2 with KOH)	CsCl 20, Cs-aspartate 110, HEPES 10, EGTA 10, MgCl ₂ 1.0, Mg ₂ ATP 5, GTP 0.1, phosphocreatine 5 (pH 7.2 with CsOH)

Figure 1

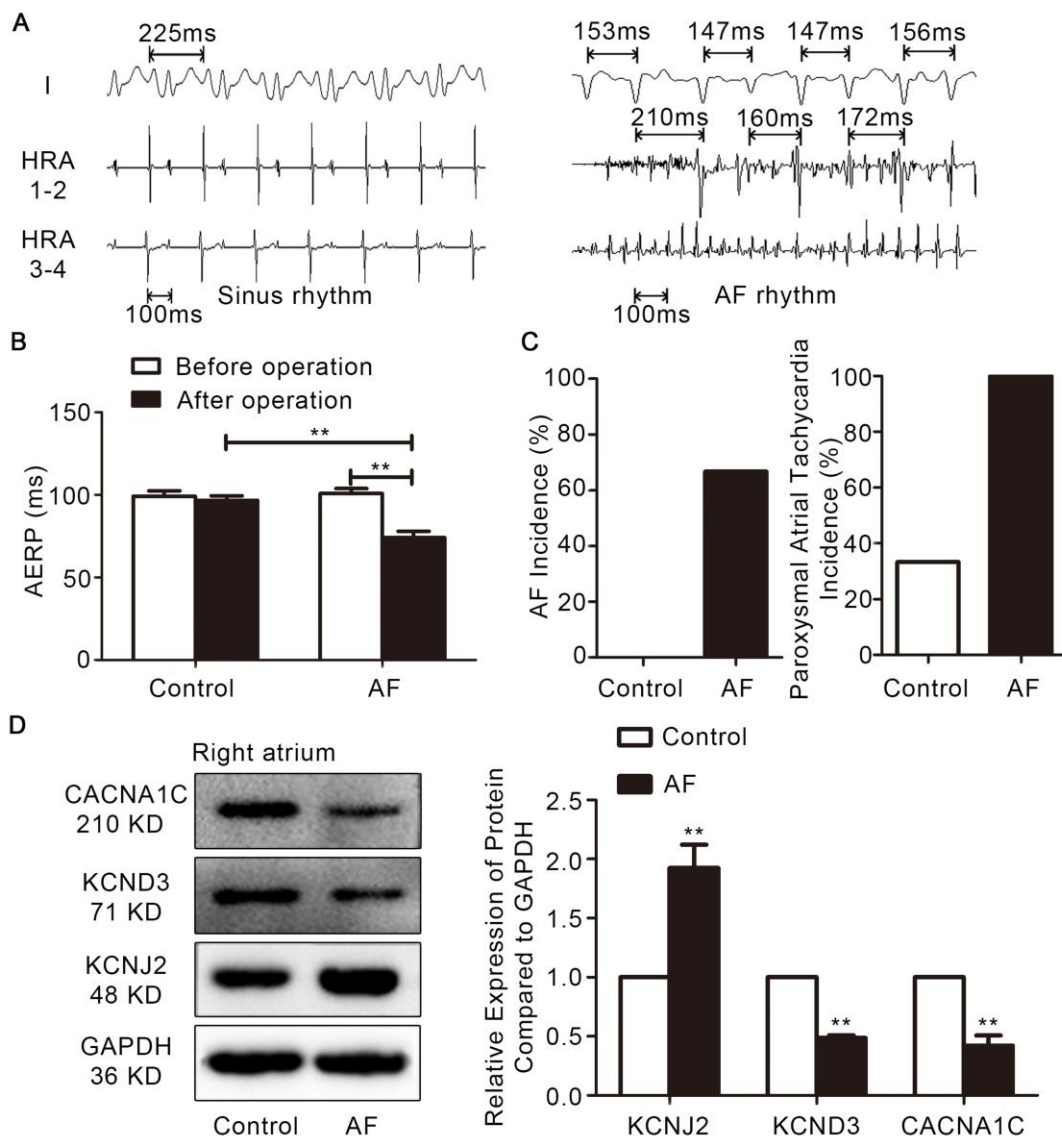


Figure 2

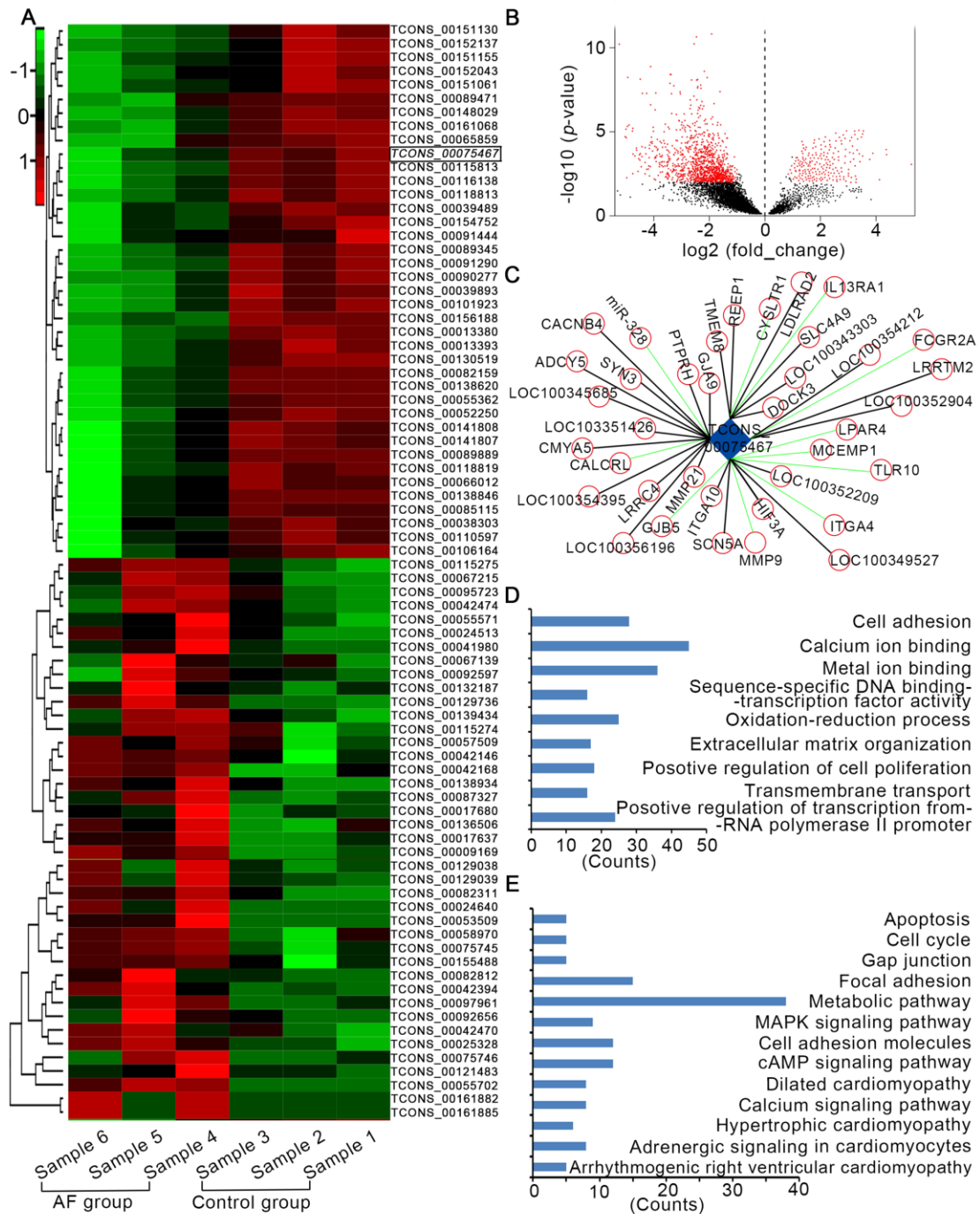


Figure 3

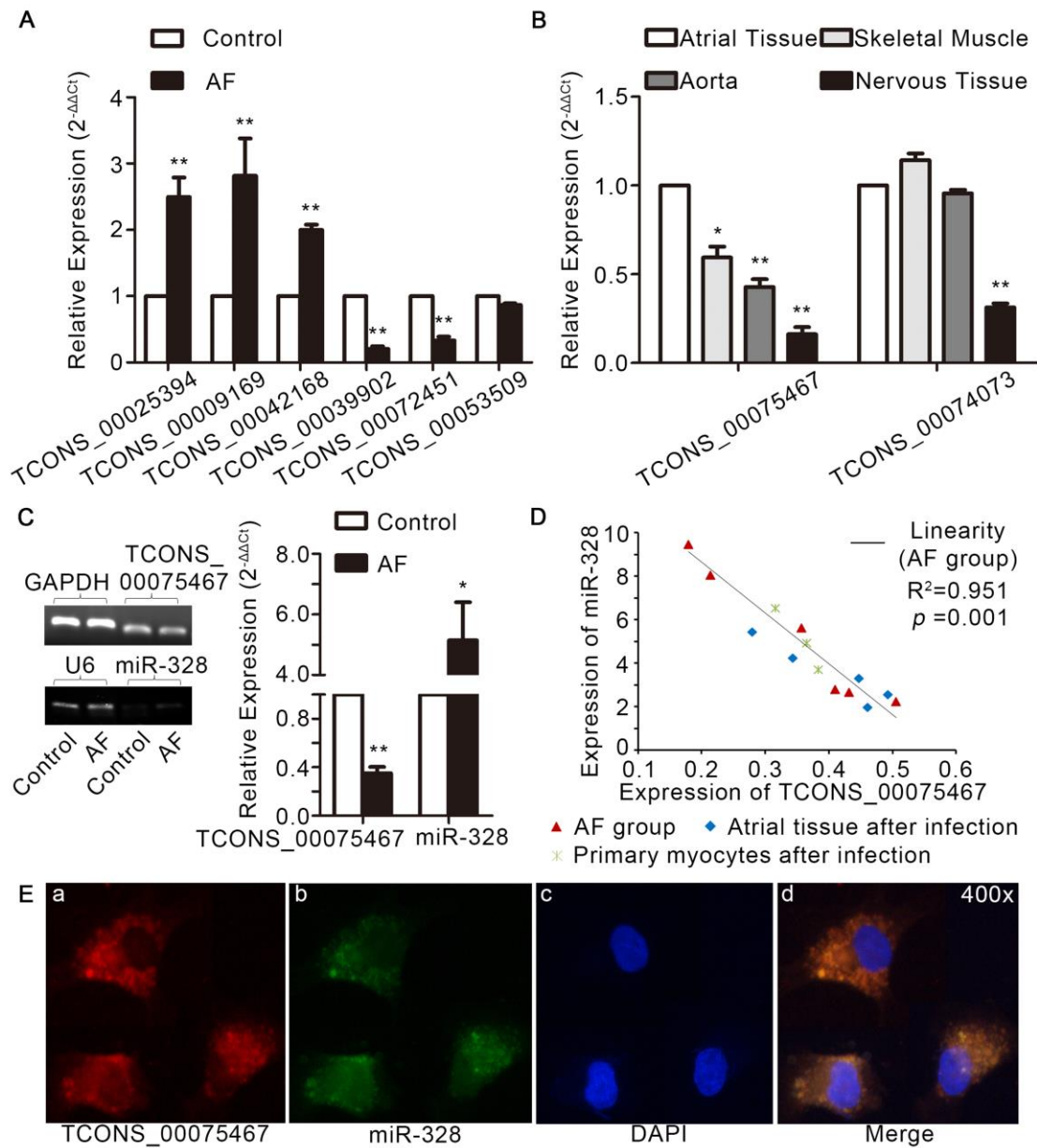


Figure 4

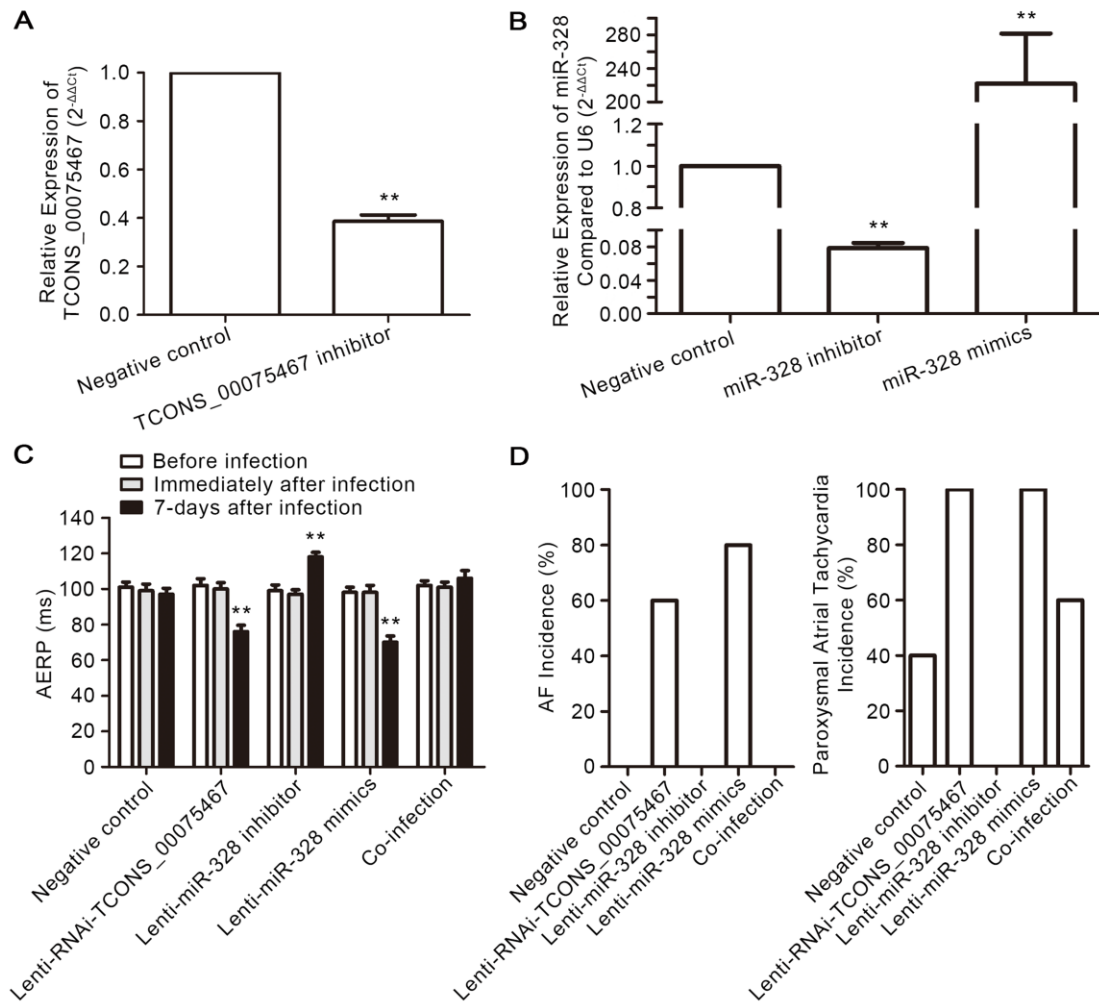


Figure 5

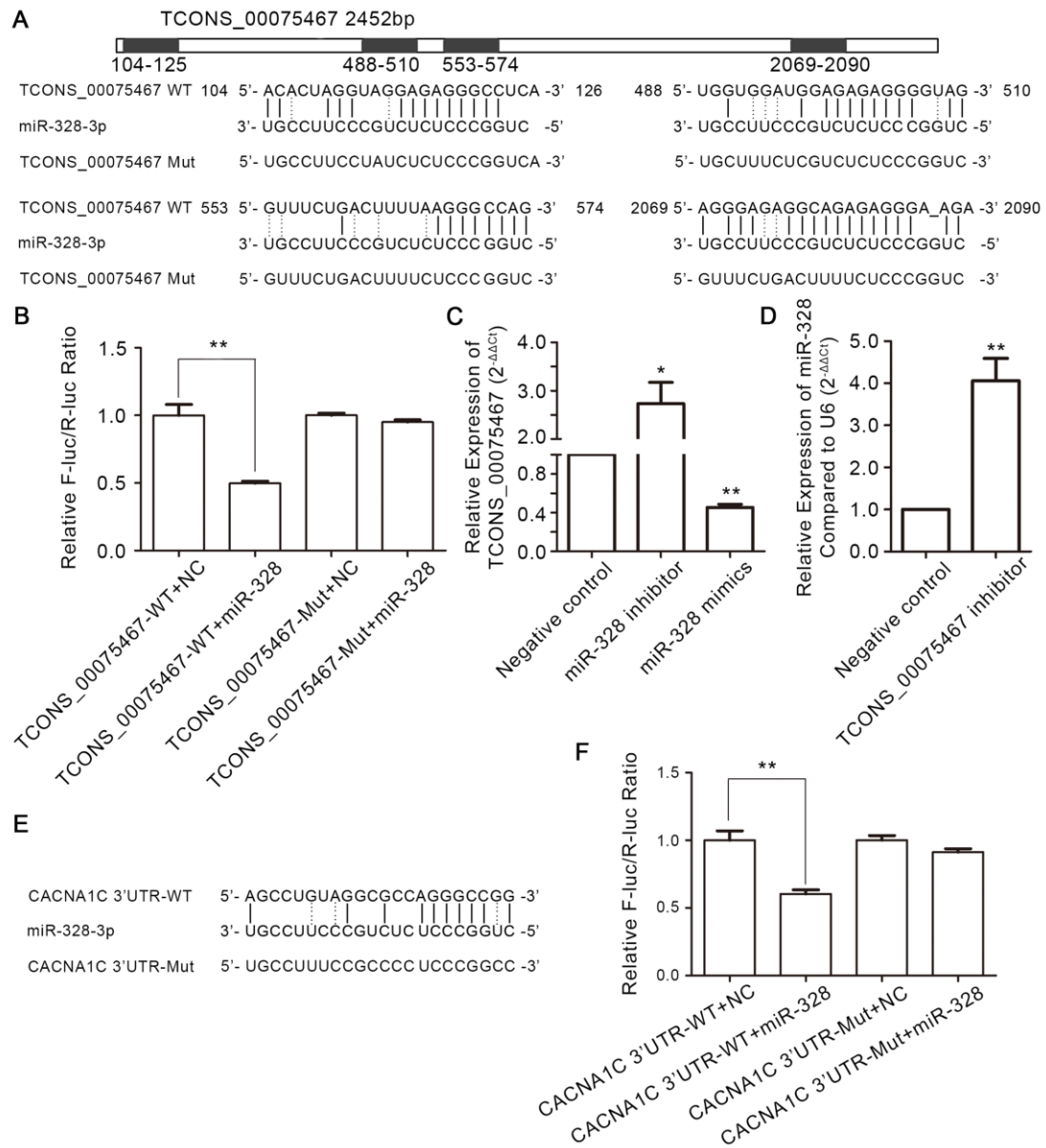


Figure 6

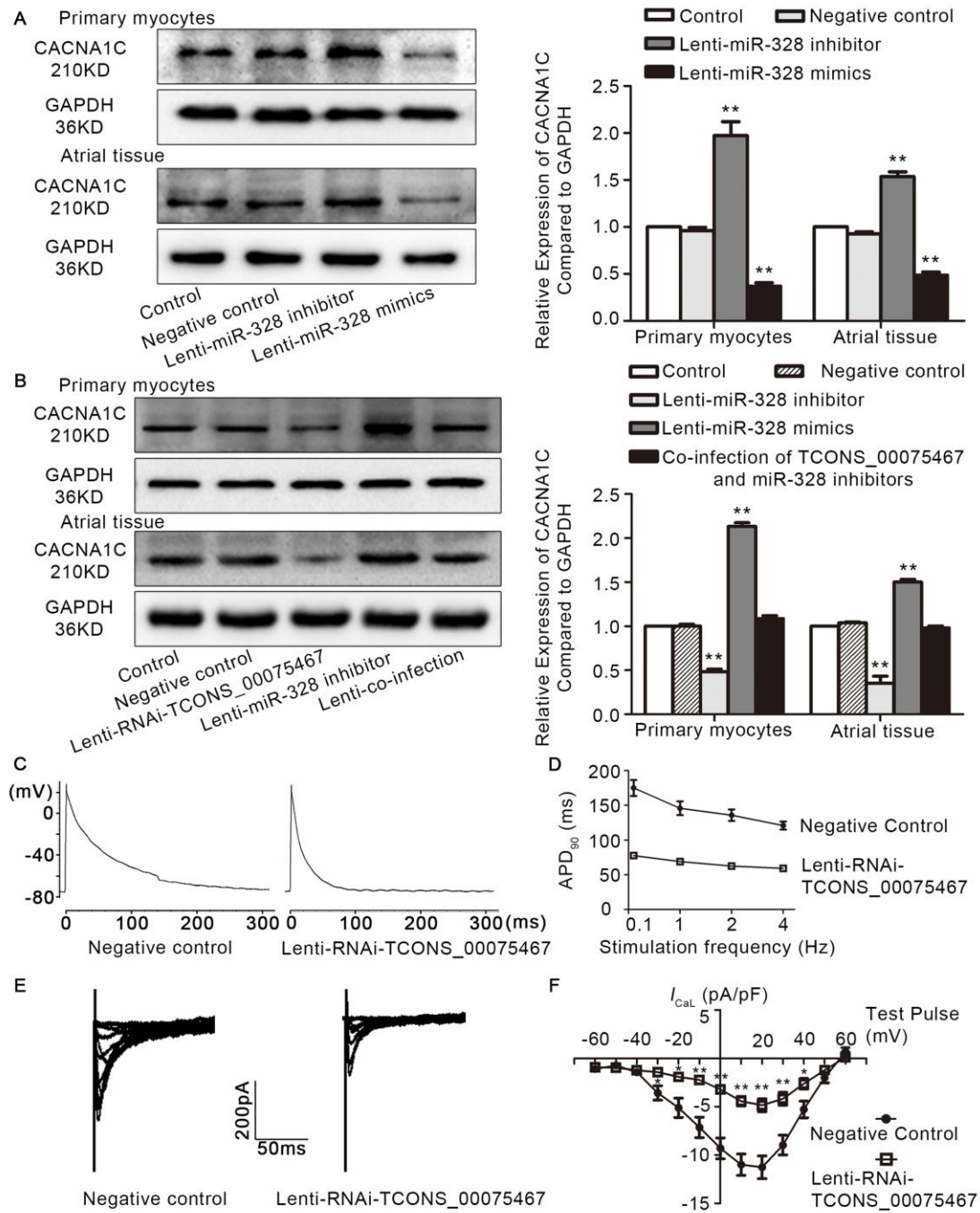


Table 1 Sectional Significant Fold Changes of the New DETs in Rabbit Models of AF

lncRNA Transcript ID	Log ₂ FC	P Value	FDR	lncRNA Transcript ID	Log ₂ FC	P Value	FDR
TCONS_0015 1130	- 1.681308 614	0.00049 6319	0.00629 1874	TCONS_0011 5275	1.71505 9139	0.00024 1285	0.00370 9978
TCONS_0015 2137	- 1.496560 931	0.00191 0665	0.01625 8616	TCONS_0006 7215	1.55946 527	0.00108 1329	0.01089 0888
TCONS_0015 1155	- 1.521575 151	0.00075 2711	0.00843 6848	TCONS_0009 5723	1.46698 2154	0.00504 4696	0.03160 8736
TCONS_0015 2043	- 1.331456 327	0.00848 0939	0.04507 2918	TCONS_0004 2474	1.59368 9225	0.00230 9321	0.01841 1526
TCONS_0015 1061	- 1.644518 333	0.00085 1183	0.00917 6648	TCONS_0005 5571	1.21953 3343	0.00800 3922	0.04328 8733
TCONS_0008 9471	- 1.278686 123	0.00453 5651	0.02928 5862	TCONS_0002 4513	1.70205 4833	0.00056 1877	0.00685 2453
TCONS_0014 8029	- 1.488826 898	0.00047 9957	0.00614 1169	TCONS_0004 1980	2.33148 212	3.31E- 05	0.00088 3525
TCONS_0016 1068	- 1.318717 915	0.00235 542	0.01866 6439	TCONS_0006 7139	1.85637 6861	0.00845 0431	0.04494 711
TCONS_0006 5859	- 1.426179 655	0.00347 3319	0.02440 9959	TCONS_0009 2597	2.08008 8715	0.00641 4902	0.03729 8092
TCONS_0007 5467	- 1.404505 813	0.00042 7815	0.00564 8726	TCONS_0013 2187	2.09174 8264	0.00160 0527	0.01436 8413
TCONS_0011 5813	- 1.464785 396	0.00020 8438	0.00333 7789	TCONS_0012 9736	1.97498 4393	0.00080 7694	0.00886 9791
TCONS_0011 6138	- 1.188611 864	0.00308 1949	0.02253 4215	TCONS_0013 9434	1.75913 0495	0.00458 3478	0.02950 013
TCONS_0011 8813	- 1.198354 714	0.00184 1108	0.01584 2514	TCONS_0011 5274	1.71536 3916	0.00832 0845	0.04445 9397
TCONS_0003 9489	- 1.500274 277	0.00059 6779	0.00716 6857	TCONS_0005 7509	1.79198 9272	0.00151 2798	0.01379 1204
TCONS_0015 4752	- 1.362692 702	0.00170 3171	0.01500 8122	TCONS_0004 2146	1.61125 8116	0.00293 8022	0.02179 6988
TCONS_0009 1444	- 1.401296 036	0.00478 6884	0.03045 3125	TCONS_0004 2168	2.12723 9216	0.00017 0719	0.00289 2472
TCONS_0008 9345	- 1.883426 317	1.32E- 06	7.75E- 05	TCONS_0013 8934	1.72054 7798	0.00152 1608	0.01383 4007
TCONS_0009 1290	- 1.935936 628	1.74E- 06	9.51E- 05	TCONS_0008 7327	1.48059 9336	0.00317 8196	0.02301 5668
TCONS_0009 0277	- 2.298169 434	2.59E- 08	3.58E- 06	TCONS_0001 7680	1.49538 3396	0.00706 241	0.03970 7897

TCONS_0003 9893	- 1.665148 981	4.57E- 05	0.00112 4709	TCONS_0013 6506	1.97380 4435	0.00240 654	0.01895 6597
TCONS_0010 1923	- 1.876396 736	3.59E- 06	0.00016 5428	TCONS_0001 7637	2.43077 9969	0.00033 6102	0.00472 5473
TCONS_0015 6188	- 2.307328 66	1.66E- 08	2.48E- 06	TCONS_0000 9169	2.44741 2817	0.00080 2863	0.00883 9557
TCONS_0001 3380	- 1.677679 112	1.65E- 05	0.00052 627	TCONS_0011 4278	1.25444 6274	0.00185 0986	0.01589 1767
TCONS_0001 3393	- 1.900585 632	2.58E- 05	0.00073 8619	TCONS_0010 2121	1.24315 6418	0.00212 1895	0.01741 0633
TCONS_0013 0519	- 2.201397 919	2.96E- 07	2.37E- 05	TCONS_0002 5394	1.47349 45	0.00040 62	0.00544 57
TCONS_0008 2159	- 1.652782 799	2.34E- 05	0.00068 6616	TCONS_0004 2470	2.58789 8428	0.00719 0968	0.04017 962
TCONS_0013 8620	- 1.595660 271	6.92E- 05	0.00153 7377	TCONS_0002 5328	3.77704 8686	0.00044 097	0.00577 7621
TCONS_0005 5362	- 1.267040 254	0.00125 7115	0.01209 2935	TCONS_0007 5746	5.27546 1096	0.00087 9099	0.00937 8859
TCONS_0005 2250	- 1.591911 434	0.00012 8118	0.00237 2045	TCONS_0012 1483	4.12660 2262	0.00703 2654	0.03960 683
TCONS_0005 3509	- 1.344172 823	0.00021 908	0.00345 7456	TCONS_0005 5702	7.20827 6521	3.25E- 07	2.56E- 05

TCONS_00075467 is highlighted in bold.

Highlights

- To identify the role of right atrial electrical remodeling in the initiation and maintenance of AF.
- The profiles of significantly expressed lncRNAs of right atria in AF and non-AF rabbit models by using high-throughput RNA-Seq were illustrated.
- The AF electrical remodeling related lncRNA was identified through bioinformatics analysis. The novel lncRNA TCONS_00075467 was demonstrated to have important biological effects on atrial electrical remodeling during AF.
- TCONS_00075467 could modulate atrial electrical remodeling by sponging miR-328 as a ceRNA to regulate CACNA1C expression.